ELECTROCHEMISTRY OF LANTHANUM IN ROOM TEMPERATURE IONIC LIQUID EMIM-DCA

A Thesis

Presented in Partial Fulfillment of the Requirements for the

Degree of Master of Science

with a

Major in Material Science and Engineering

in the

College of Graduate Studies

University of Idaho

by

Ian C. Ehrsam

Major Professor: Batric Pesic, Ph.D.

Committee Members: Indrajit Charit, Ph.D.; You Qiang, Ph.D.

Department Administrator: Eric Aston, Ph.D.

May 2018

AUTHORIZATION TO SUBMIT THESIS

This thesis of Ian C. Ehrsam, submitted for the degree of Master of Science with a major in Material Science and Engineering and titled "ELECTROCHEMISTRY OF LANTHANUM IN ROOM TEMPERATURE IONIC LIQUID EMIM-DCA," has been reviewed in final form. Permission, as indicated by the signatures and dates below, is now granted to submit final copies to the College of Graduate Studies for approval.

Major Professor: ___________________________________ Date: ______________

Batric Pesic, Ph.D.

Committee Members: ___________________________________ Date: ______________

Indrajit Charit, Ph.D.

___________________________________ Date: ______________

You Qiang, Ph.D.

Department

Administrator: ___________________________________ Date: ______________

Eric Aston, Ph.D.

ABSTRACT

In nuclear engineering, the accumulation of lanthanides, as the main fission products, has detrimental effects on the efficiency of nuclear fuel because of strong neutron absorption properties. Therefore, the lanthanides need to be separated from actinides, a difficult task due to the similarity of chemical and electrochemical properties. One of the avenues for reprocessing nuclear fuels is electrometallurgy from ionic liquids. Ionic liquids can be classified according to temperature of application into (1) high temperature and (2) low temperature. High temperature ionic liquids are eutectic inorganic salts, such as LiCl-KCl. They are operational in the range 400 – 600 °C. Low temperature ionic liquids are made of an organic (cation) and inorganic (anion) components. They are fully ionized, stable, conductive and liquid in a much lower temperature range than ionic liquids based on inorganic salts, typically 25 - 100 °C. For that reason, they are often termed as room temperature ionic liquids (RTILs).

Due to lanthanide's large electronegative deposition potential (~ -2.4 V vs SHE) traditional aqueous electrodeposition processes cannot be used as hydrogen evolution from water occurs prior to any lanthanide metal deposition. RTIL's provide a unique solution to this problem as these salts are liquid at room temperature and provide a wide electrochemical window (up to 5 V) for deposition of electronegative metals without the detrimental effects from hydrogen ion reduction, as present in aqueous systems.

The goal of this study was to examine the electrochemistry and deposition morphology of lanthanum metal in the RTILs 1-ethyl-3- methylimidazolium dicyanamide (EMIM-DCA) and 1-butyl-3-methylimidazolium dicyanamide (BMIM-DCA) ionic liquids. These particular RTILs are stable in the cathodic direction up to -2.4V vs Ag/AgCl, providing the adequate stability to observe the electrodeposition of lanthanum metal.

Reduction mechanisms were characterized on the basics of cyclic voltammetry technique. For the determination of kinetic parameters, such as diffusion rate constant and reaction rate constant the rotating disk technique was employed. The effects of water and ethanol concentration were studied in details. The role of water was important to determine in order to evaluate its effect during its eventual absorption from open atmosphere. Ethanol gained in importance because of the solubility of rare earth salts in alcohols, as the only viable route toward solubilization of rare earths in ionic liquids. The diffusion coefficient of water in EMIM-DCA was calculated to be 7.6x10^{-7} cm^{2}/sec. The reduction of water on platinum in EMIM-DCA exhibited sluggish kinetics and the rate constant was calculated to be 2.15x10^{-5} cm/sec. Both water and ethanol additions slightly reduced the stability window of the RTIL.

Morphology of lanthanum electrodeposits, observed around -2.0V, was characterized by using scanning electron microscope (SEM). Thin dense films were generally produced. However, the organic components of ionic liquids were also intermixed with metallic deposit, which were removed by washing with alcohol.

ACKNOWLEDGMENTS

During my research work, I have benefited from the interactions with my professors, colleagues and friends. Their help and encouragement was invaluable. I would especially like to express the deepest appreciation to my advisor, Dr. Batric Pesic. Without his guidance and persistent help, this thesis would not have been possible. He not only taught me to do research, but also provided me personal examples of scientific diligence and integrity.

Second, I would like to express my thanks to all of my committee members, Dr. Indrajit Charit and Dr. You Qiang, for their encouragement and assistance during my graduate studies.

Third, Financial support for this work was funded by the U.S. Department of Energy for funding the research through the Nuclear Energy Universities Programs (NEUP PROGRAM, Contract No. DE-NE00008556).

Finally, I would like to thank the University of Idaho for giving me a treasured opportunity to further my study and lead me into a whole different life. Needless to say this place has generated many lingering memories for me to treasure for a lifetime.

DEDICATION

To my beloved family for their continuous support all through these years. My family has given me encouragement and support, and without them I would not be who I am today. I would also like to express my gratitude to all those who helped me during the writing of this thesis.

TABLE OF CONTENTS

Authorization to Submit Thesis ii
Abstract iii
Acknowledgments v
Dedication vi
Table of Contents vii
List of Figures ix
List of Tables xi
CHAPTER 1 INTRODUCTION 1
    1.1 Room Temperature Ionic Liquids 2
        1.1.1 Classification of Ionic Liquids 3
            1.1.1.1 Generation I 4
            1.1.1.2 Generation II 5
            1.1.1.3 Characterization of Ionic Liquids by Acidic and Basic Behaviors 5
        1.1.2 Properties of Ionic Liquids 6
            1.1.2.1 Electrochemical Windows 6
            1.1.2.2 Density 7
            1.1.2.3 Viscosity 7
            1.1.2.4 Conductivity 8
            1.1.2.5 Solvation and Solubility 8
        1.1.3 Benefits and Applications of Ionic Liquids 9
        1.1.4 The Classification of Dicyanamide Ionic Liquids 10
        1.1.5 Previous Electrochemical studies form Dicyanamide Based Ionic Liquids 11
        1.1.6 Electrochemical Reduction Mechanisms for 1,3-Dialkyl-imidazoliums 11
    1.2 Electrochemistry of Lanthanides 12
        1.2.1 Thermodynamics and Half Cell Reactions of Lanthanide Electrochemistry 13
        1.2.2 Electrodeposition of Lanthanides from Ionic Liquids 15
        1.2.3 Electrochemical Behavior of Lanthanum in Ionic Liquids 16
CHAPTER 2: ELECTROCHEMICAL METHODS 17
    2.1 Cyclic and Linear Sweep Voltammetry 17
    2.2 Chronoamperometry 20
    2.3 Rotating Disk 22
CHAPTER 3: EXPERIMENTAL 25

3.1 Materials..........25
3.2 Glove Globe..........25
3.3 Electrochemical Cell..........26
3.4 Rotating Disk Setup..........27
3.5 High Temperature Setup..........28
CHAPTER 4: RESULTS AND DISCUSSION..........29
4.1 Rotating disk studies of EMIM-DCA with $LaCl_3$..........30
4.2 Studies of EMIM-DCA-$LaCl_3$ in Inert Atmosphere..........32
4.3 Effect of Ethanol Addition to EMIM-DCA with and without $LaCl_3$..........32
4.4 Effect of EMIM-DCA Addition to Ethanol with and without $LaCl_3$..........34
4.5 Effect of Water Addition to EMIM-DCA with and without $LaCl_3$..........35
4.6 Effect of Electrode Surface on BMIM-DCA with and without $LaCl_3$..........39
CHAPTER 5: SURFACE MORPHOLOGY AND CHARACTERIZATION..........41
5.1 Optical Characterization of Electrodeposited Films on a Pt Working Electrode..........41
5.2 SEM Characterization of Electrodeposited Films..........43
5.3 XRD Characterization of Electrodeposited Film on a Mo Working Electrode..........48
CHAPTER 6: FUTURE WORK..........50
CHAPTER 7: CONCLUSIONS..........51
REFERENCES..........52

LIST OF FIGURES

Figure 1.1: Common cations and anions of ionic liquids [10] 4
Figure 1.2: Three possible breakdown methods for 1,3-dialkylimidazoliums [24] 12
Figure 2.1: CV analysis of a reversible species where cathodic and anodic peaks are symmetric 18
Figure 2.2: Example of a CV of an reversible, quasi-reversible, and irreversible system 19
Figure 2.3: Representative LSV plot resulting current density vs applied potential 19
Figure 2.4: Potential versus time waveform of CA and resulting current versus time response [33]. 20
Figure 2.5: Example of a Cottrell plot for an electroactive species [33] 21
Figure 2.6: Rotating disc electrode; cross section, side and bottom view of liquid flow pattern[35]. 22
Figure 2.7: A series of voltammograms is acquired over a range of different rotation rates 23
Figure 2.8: Example of a Levich plot for a mass controlled system 23
Figure 2.9: Example of a Koutecky-Levich plot for a mass controlled system 24
Figure 3.1: Glove globe with rotating disk setup used for closed atmosphere studies [36] 26
Figure 3.2: Electrochemical cell for studies of lanthanum from EMIM-DCA-$LaCl_3$ [36] 27
Figure 3.3: Electrochemical setup for rotating disk studies of lanthanum from EMIM-DCA [36] ... 28
Figure 3.4: Electrochemical setup for high temperature deposition of La from ionic liquid [36] 28
Figure 4.1: Effect of scan range on CV of EMIM-DCA with and without $LaCl_3$ present 29
Figure 4.2: LSV of EMIM-DCA with $LaCl_3$ present. Effect of RPM and scan rate 30
Figure 4.3: Levich plot of EMIM-DCA with $LaCl_3$ 31
Figure 4.4: Koutecky-Levich plot of EMIM-DCA with $LaCl_3$ 31
Figure 4.5: CV of EMIM-DCA with $LaCl_3$ present. Inert Atmosphere vs Open to atmosphere 32
Figure 4.6: Effect of RPM on LSV of EMIM-DCA-$LaCl_3$. Inert Atmosphere 32
Figure 4.7: Effect of Ethanol addition on the CV of EMIM-DCA with and without $LaCl_3$ 33
Figure 4.8: Effect of EMIM-DCA addition on the CV of EtOH with and without $LaCl_3$ 34
Figure 4.9: Effect of H_20 addition on the CV of EMIM-DCA with and without $LaCl_3$ 36
Figure 4.10: Effect of scan rate on EMIM-$LaCl_3$ + 500 uL H_20 37
Figure 4.11: Randles Sevcik plot on reaction of EMIM-$LaCl_3$ + 500 uL H_20 38
Figure 4.12: Effect of RPM on the CV of EMIM-DCA- $LaCl_3$ with 500 uL H_20 38
Figure 4.13: Levich plot of EMIM-DCA- $LaCl_3$. with 500 uL H_20 39
Figure 4.14 :Koutecky- Levich plot of EMIM-DCA-LaC_{l3} with 500 uL H_2O 39
Figure 4.15: Effect of Electrode Surface on the CV of BMIM-DCA with and without $LaCl_3$ 40
Figure 5.1: Chronoamperometry of EMIM-DCA-$LaCl_3$ at various overpotentials 41
Figure 5.2: Optical microscopy of film developed by CA for 3 sec at various potentials 42

Figure 5.3**:** SEM images presenting surface morphology of deposit on the platinum working electrode. CA performed for 2 hours at -2.0V at 80 C. 44
Figure 5.4: SEM images captured of electrode surface after control test 45
Figure 5.5: SEM images presenting surface morphology of deposit on the glassy carbon working electrode. CA performed for 20 sec at -3.5V at room temperature 46
Figure 5.6**:** SEM images presenting surface morphology of deposit on the glassy carbon working electrode. CA performed for 1 hours at -2.0V at 80 C. 47
Figure 5.7: SEM images presenting surface morphology of deposit on the brass working electrode. CV performed 0V to -2V at 80C 48
Figure 5.8**:** XRD characterizing the surface morphology of deposit as La on the Mo working electrode. CA performed for 1 hours at -2.2V at 80 C 49

LIST OF TABLES

Table 1.1: Typical Reduction Potentials in Comparison to the Standard Reduction Potential of Lanthanum 15
Table 4.1: Limiting Current Values from LSV of EMIM-DCA with $LaCl_3$ under Different Rotation Speeds and Scan Rates 31
Table 5.1: Two Theta Values for HCP Lanthanum [40] 49

CHAPTER 1: INTRODUCTION

Lanthanides are commonly used in batteries and hard drives due to their interesting optical, electric, and magnetic storage properties. Lanthanides are highly electronegative, with reduction potentials typically below -2.0V. For example, cerium and lanthanum have reduction potentials about -2.4 V vs SHE. According to the thermodynamics of electrochemistry, an electrode must have a reduction potential lower than the standard potential of a metal in question in order for the metal to be reduced. In aqueous solutions, water has a reduction potential between 0 and -0.8 V vs SHE which means the metals with lower standard potentials, such as lanthanides, cannot be reduced. The electrodeposition of lanthanides, therefore is commonly performed in high temperature molten salts, or organic solvents. While molten salts and organic solvents perform well, they have many economic and environmental drawbacks. Molten salts are highly corrosive and not very cost efficient due to their high temperature operation. While organic solvents can be run at room temperature, they are very volatile. An alternative to both organic solvents and molten salts is room temperature ionic liquids (RTIL) because of their wide electrochemical stability windows, high chemical stability, ionic conductivity, and high solubility.

While electrochemistry of lanthanides in ionic liquids has been of interest to researchers for many years, this subject has not been fully studied. Published literature currently has conflicting information on the electrochemical reduction of lanthanides in ionic liquids. Therefore, more research is needed either to confirm or deny previous information.

The objective of this research was to examine the electrochemistry of lanthanides in the DCA RTILs particularly the reduction of lanthanum. The ionic liquids used for this study were EMIM-DCA and BMIM-DCA where EMIM stands for 1-ethyl-3- methylimidazolium, BMIM stands for1-butyl-3- methylimidazolium and DCA stands for dicyanamide. Dicyanamide based ionic liquid was selected over other ionic liquids because it has more efficient mass transfer, higher solubility and low viscosity as compared to other ionic liquids. EMIM-DCA ionic liquids also have been reported to have a flexible solvating ability because its basic anion dicyanamide which enables EMIM-DCA to dissolve a wide range of both organic and inorganic salts. Another important characteristic is that DCA ionic liquids are stable in open atmosphere and moisture resistant, making them suitable for industry.

The effects of water and ethanol on the electrochemistry of EMIM-DCA with and without lanthanum were also desired. Ionic liquids are known to absorb water from atmosphere, interrupting film formation, therefore the tolerance and stability of EMIM-DCA with water should be understood. Ethanol is a common organic solvent used in traditional processes, because ethanol helps to dissolve the metal salts into ionic liquid. The study of how the EMIM-DCA tolerates addition of ethanol should also be understood. Another major objective of this research was to characterize and observe the morphology of lanthanum films from DCA RTILs.

1.1 Room Temperature Ionic Liquids

Studies on room temperature ionic liquids (RTILs) started a long time ago. Walden [1] first reported on a room temperature molten salt in 1914. According to his report, ethyl-ammonium nitrate was prepared from chemical reaction between the ethylamine and concentrated nitric acid. Other RTILs were later prepared by mixing the warm 1-ethyl pyridinium chloride with aluminium chloride as reported by Hurley and Weir [2]. In 1970s and 1980s, research on RTILs from organic chloride-aluminium chloride ($AlCl_3$) were carried out by Osteryoung et al., [3] and Hussey et al., [4 . RTILs were developed for various applications and became popular in the last decade due to their expanded range of applications in different fields, particularly in electrochemical applications. RTILs are used as electrolytes in lithium ion rechargeable batteries, fuel cells, capacitors, solar cells, and actuators [5]. In metal industries, the range of important metals such as Li, Na, Ti, Al studies were difficult to perform or even impossible to conduct using aqueous electrolyte until RTILs were produced [6].

Ionic liquids are generally defined as ‘a liquid consisting solely of cations and anions with a melting point of 100 °C and below’ [7]. RTILS are ionic liquids with a melting point between 25 and 100°C. When compared to classical molten salts, ionic liquids are less corrosive and easier to handle. Cations and anions are the main components for ionic liquids, which influence different parameters. The physical properties of ionic liquids are controlled by the cations. The stability and chemical reactivity of ionic liquids are influenced by the anions. Anions and cations are specified by the application of the IL. For electrodeposition, a specified range of anions and cations is used. For electrochemical studies on metals, anions such as $AlCl_4$, $SnCl_2$, BF_4, PF_6, Tf_2N, $ZnBr_2$, $ZnCl_2$, $NiCl_2$, $NbCl_5$ and DCA were used.

The anions and cations for metal study were chosen according to the nature of the ionic liquid required for the particular metal deposition. These anions and cations also influence the physical properties, like viscosity and conductivity of the electrolyte [8]. Generally, cations are bigger in size than the anions. Low symmetry cations from organic species result in ionic liquids with lower melting points. The chain length of the cation also influences the melting point of the ionic liquid. The radii of the cations influence the viscosity of ionic liquids and as a result this influences the mass transport of the metal ions [8]. For electrodeposition, ionic liquids with small and less symmetric anions are favorable because of their viscosity. The negative charge of less symmetric anions does not participate in the hydrogen bonding, and therefore creates low viscosity ionic liquids. The proportion of anions to cations, reduction potential and nucleation process of the metal ions also can be controlled [9]. Depending on the acidic, basic or neutral nature of the ionic liquid, it is likely for us to predict the possibility of the reduction of a particular metal [9]. This means the nature of the ionic liquid depends on the proportion of anion and cation used. Thus, ionic liquids used for electrodeposition can be classified in several groups depending on their nature and behavior.

1.1.1 Classification of Ionic Liquids

Technically any salt above its melting point is an ionic liquid. This means molten salts such as NaCl with a melting point of 800 C are ionic liquids. The general definition for ionic liquids, is any ionic material consisting of entirely of ions that are liquid below 100 C. RTILs are ionic liquids that are liquid between 25 to 100 C. Ionic liquids are semi-organic because their cations are substituted with different asymmetrical bulky groups. These bulky groups prevent the packing of the ions into a crystal. Ionic liquids are characterized further by generations and acidic/basic behaviors.

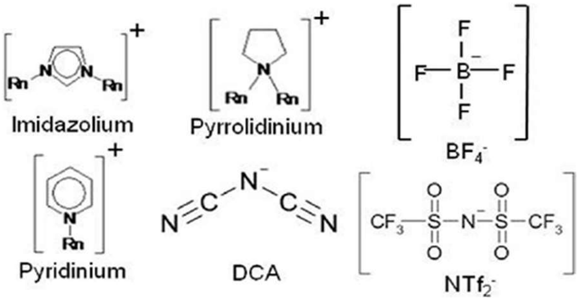

Figure 1.1: Common cations and anions of ionic liquids [10].

1.1.1.1 Generation I Ionic Liquids

The first generation of ionic liquids were mainly composed of cations like dialkylimidazolium and alkylpyridinium, and anions like chloroaluminate and other metal halides [11]. Ionic liquids with these common metal halide anions react with water and oxygen, so they must be handled under inert-gas atmosphere [4]. In the 1980s, Hussey et al., [4] started extensive research on first generation ionic liquids. However, due to these limitations, the progress and their use was limited. For this reason, research was directed towards the synthesis of air and water-stable ionic liquids, also known as the second generation of ionic liquid.

1.1.1.2 Generation II Ionic Liquids

Generation II are Lewis neutral ionic liquids where their cations are based on weak acids and anions are based on weak bases [12]. Common anions are BF_4^- , PF_6^- , SCN and SbF_6^- and the cations are based on imidazolium, pyridinium and quaternary ammonium salts [12]. These ionic liquids are air and water stable ILs [12-14]; however, long time exposure to water can have serious effects on the properties of these ionic liquids [12] .The preparation of these ionic liquids takes place in two steps, alkylation of the organic base and anion exchange [12]. For these ionic liquids preparation is possible at room temperature, but application is possible only at elevated temperature [6]. Due to choice of cations like ethyl-imidazolium, the formed ionic liquids have low viscosity and high conductivity [13]. One of the disadvantages of these ionic liquids is the high cost. According to Gorke et al. [14], the high costs are related to starting materials (namely fluorinated components) and purification of final product required in the preparation. The most important disadvantage of the second generation is the toxicity, which in general is similar to those of chlorinated and aromatic solvents [14].

1.1.1.3 Characterization of Ionic Liquids by Acidic and Basic Behavior

The acidity or basicity of ionic liquids is governed by the ionic bond strength or how the cation and anion combine. For combinations, the acidic characteristic depends on whether the combination is Lewis, Bronsted-Lowry or a combination of both. Lewis ionic liquids depend on the deficiency of their electrons. The electrons accepting abilities can be located in the anion or cation. The most common Lewis acidic controlled ionic liquids are haloalumiate ILs (first generation ionic liquids). For haloaumuite ionic liquids the mole fractions of $AlCl_3$ define the ILs as either basic (less than 0.5), acidic (more than 0.5), or neutral.

The acidity of Bronsted-Lowry combined ionic liquids is controlled by ionizable protons. A Bronsted acid ionic liquid (protic) is an ionic liquid that denotes its hydrogens or protons easily.

Bronsted basic ionic liquids readily accept hydrogens or protons easily. Examples of Bronsted-Lowry basic ionic liquids would be ionic liquids with anions such as acetate, or dicyanamide, which are known as stronger acceptors for protons than water. This means that water will partly dissociate, producing OH in basic ionic liquids.

Neutral ionic liquids have anions that can be described as neutral in the acid/base sense or very weakly basic. These ionic liquids exhibit only weak electrostatic interactions between the cation and anion, thus imparting advantageously low melting points and viscosities. Included in this class are anions such as hexafluorophosphate, bis(trifluoromethanesulfonyl)amide (TFSI) and tetrafluoroborate [15]. Neutral ionic liquids typically exhibit good thermal and electrochemical stability, and therefore are often utilized as inert solvents in a wide range of applications.

1.1.2 Properties of Ionic Liquids

Ionic liquids exhibit a unique variety of electrochemical and physicochemical properties, such as low melting points, wide electrochemical windows and good conductivity. Ionic liquids are used in both organic and inorganic synthesis, which makes them both energy and cost effective. This made RTILs a focal point of “green” chemistry [16] and stimulated interest in academia.

1.1.2.1 Electrochemical Window (Potential Range)

The electrochemical window is defined by the potential difference between the reduction of the organic cation and the oxidation of anion. The electrochemical window is one of the most important features for an electrolyte used in electrochemical studies. It is important to know potential limits for the reduction of cation and the oxidation of anion, because if the applied potential difference is larger than the potential range, the electrolyte will decompose to other products. For example, EMIM-DCA breaks down at around -1.8 V vs Ag/AgCl on platinum, and forms a neutral dimer (NCN_3)[17].

Most RTILs have electrochemical windows above 3 V, which are wider than most aqueous solutions and conventional organic solvents. The size of the range depends on the constituent cations and anions. For example, imidazolium based ionic liquids have slightly narrower ranges, usually around one volt less, because of the easy reduction of the imidazolium cation. When imidazolium cation is replaced by the harder to reduce quaternary cations, the potential range becomes much wider. Anions can also influence potential range but are more likely to affect the solvation structure, ionic conductivity, and viscosity. The potential range can also be narrowed by additives such as water and ethanol.

1.1.2.2 Density

Density is the most frequently reported property for ionic liquids because it provides information on the molar volume and other derived properties. The densities of ionic liquids generally lie in the range of 1 to 1.6 g cm^{-3}, which are mostly higher than those of organic solvents and water [16]. The densities of ionic liquids strongly depend on the constituent cations and anions. For an imidazolium cation, the density decreases by increasing the length of the alkyl chain due to the poor crystal packing in the bulky cation [16]. However, for most ionic liquids, increasing the molecular mass of the anion increases the density.

1.1.2.3 Viscosity

Viscosity is a measurement of the resistance of a fluid to flow under the influence of gravity. Viscosity has a strong effect on the rate of mass transport within solutions which makes it a very important property for electrochemistry. The inverse of viscosity is called fluidity. Most RTILs are viscous liquids with viscosities in the range of 30-450 cP, which are generally 1-3 orders of magnitude greater than those of conventional organic solvents [16]. Anions affect viscosities according to their ability to participate in hydrogen bonding. Generally, ionic liquids with larger anions have higher viscosities because of their greater hydrogen bonding strength. The high viscosity of an ionic liquid is related to van der Waals interactions, hydrogen bonding, and electrostatic factors. For example, increasing the length of the organic cation alkyl chain increases the van der Waals interactions, therefore increasing the viscosity. Viscosities can be significantly changed by adding small amounts of organic solvents, water, or other diluents [17]. The viscosities of ionic liquids are also highly temperature dependent.

1.1.2.4 Conductivity

Conductivity is a measurement of the ability of a material to pass electric current. The inverse of conductivity is resistivity. Ionic liquids are often used as solvents to study electrochemistry as reported here, so like viscosity, conductivity is also an important property. There are two different terms to describe the conductivities of ionic liquids: specific conductance and molar conductance. Specific conductance is related to the molar conductance by the following expression:

$$\Lambda = M/\rho \quad \text{(Eqn. 1.1)}$$

where M is the molar weight of the ionic liquid of interest, Λ is specific conductance, and ρ is molar conductance. Ionic liquids consist entirely of ions and include an abundance of charge carriers, so they are expected to have high electrical conductance. However most ionic liquids display an electrical conductance similar to that of organic solvents with added electrolytes, and its conductance even lower than water containing dissolved salts [18]. Ionic liquids have small conductivities because of their high viscosities and large ion sizes, which greatly reduces their mobility. Generally, the conductivity is inversely proportional to viscosity, which means an increase in viscosity would result in a decrease in conductivity.

1.1.2.5 Solvation and Solubility

The solvation of ionic liquids is very important for both fundamental and applied studies. Ionic liquids can be regarded as polar solvents, as they solely consist of ions. However, they dissolve both polar and non-polar solutes. The polarity of solvents is a very important factor as it enables one to determine an ionic liquid’s ability to dissolve a certain solute; therefore, it is defined as the solvation capability. In some cases, the solubility of some salts in ionic liquids is low due to the weak coordinating ability of the bulky cations and anions forming ionic liquids. This can also hinder the breakdown of the electrostatic interactions between metal salts. However, if the temperature of the system is increased, the solubility of salts is often enhanced. Changing the ionic liquid polarity is also an important factor that helps to increase the solvation ability. By reducing the alkyl chain length in the cation, the polarity of the ionic liquid will increase and its ability to dissolve polar compounds will also increase. Therefore, using ionic liquids with long alkyl chains will reduce the polarity but the liquids will become more suited to dissolve non-polar compounds.

1.1.3 Benefits and Applications of Ionic Liquids

Ionic liquids are suitable for many applications, including catalysis and surface chemistry, nuclear fuel reprocessing, liquid/liquid extractions, electroanalytical applications and different processes in chemical industry. The potential of ionic liquids as electrolytes in electrochemistry is based on their nonflammability, high ionic conductivity, viscosity and electrochemical and thermal stability. Thus, ionic liquids are used in batteries, capacitors, fuel cells, photovoltaics, actuators, and electrochemical sensors [8]. Furthermore, ionic liquids enable the electrochemical deposition of noble metals, alloys and also of conducting polymers [8].

For lanthanides, ionic liquids have potential applications in their electrodeposition, especially RTILs. The electrochemical properties of an RTIL can be exploited by simply electrodepositing lanthanide onto the working electrode. This can also be used to study the formation and behavior of lanthanides. In aqueous solutions, studies and deposition of lanthanides cannot be performed because the electrochemical window is limited by the oxidation of water and reduction hydrogen. As mentioned in the last section, ionic liquids have large potential windows. These large windows can be used in separations by removing species from RTIL through the selection of deposition potential. If more than one species is present and needs to be removed, then different deposition potential could be used to remove them individually from the ionic liquid. Impurities like ethanol and water may have effects on the system, but overall ionic liquids remain stable.

RTILs have a vast number of potential combinations that can assist in meeting a variety of anticipated uses. A major advantage of ionic liquids is that they have the ability to be repeated in cycles of extraction and electrodeposition and can also be recycled for later use. This allows one to the ability to study electrochemical and formation of morphology of metals like lanthanides. Despite such advantages and research, ionic liquids have not been fully exploited in electrodeposition technologies. Rotating disk studies, for example, have not been applied to most systems of ionic liquids. The cause for this slow development could be the higher costs of solutions, stability of the solvents in atmosphere, transport problems such as high viscosities, or the stability of the metal phase.

1.1.4 The Classification of Dicyanamide Based Ionic Liquids

Ionic liquids based on dicyanamide (DCA) anion have been synthesized and characterized by many authors. With DCA anion, high fluidity and conductive ionic liquids are made by combining heterocyclic cations, such as 1,3-dimethylimidazolium and 1-ethyl-3-methylimidazolium. Hydroxyl ILs that contain DCA anion exhibit comparable polarity, and are moderately higher than those of their nonhydroxyl ILs [14]. There are several series of salts based on the DCA anion, such as quaternary ammonium, pyrrolidinium, and imidazolium dicyanamides [15], most of which are liquids at room temperature. Since DCA is a strong liquid and acceptor of protons, ionic liquids made with DCA usually are basic ionic liquids [14].

1.1.5 Previous Electrochemical Studies from Dicyanamide Based Ionic Liquids

DCA based ionic liquid have more efficient mass transfer, higher conductivity and solvation compared to other ionic liquids. DCA ionic liquids are also known to be stable in open atmosphere and are moisture resistant. Other researchers have studied DCA ionic liquids for the electrodeposition of a variety of metals. Deng et al.,[19] electrodeposited many metals; including Al, Mn, Sn, Zn, Ni, and Cu from EMIM-DCA. They noticed that metallic Cl readily dissolved in the ionic liquid due to the strong complexing ability of DCA toward transition metals. Liu et al., [20] performed electrochemical studies of in(III) in [BMP]+[DCA] using $InCl_3$ as the source of In. Static voltammetry and convective RDE voltammetry were used determine to parameters, such as the diffusion coefficient and formal potential of In species. The contrasted electrochemical behavior of Cu ions in [BMIM][DCA] ionic liquid was discovered by Beuss-Herman et al.,[21]. Simons et al,. [22] examined the effect of water concentration on Zn electrochemistry in [emim][dca] + 10 mol % Zn(dca)2. They noted as the potential was scanned in the negative direction, all three voltammograms show a single clear reduction peak; regardless of the amount of water added, the reoxidation of the deposit was hindered.

1.1.6 Electrochemical Reduction Mechanisms for 1,3-Dialkyl-imidazoliums

The reduction of 1,3-dialkylimidazoliums, EMIM and BMIM, generally takes place at around −1.8 to −1.9V vs. Ag/AgCl, and examples of voltammetry for these ILs are abundant in the literature. The C2 carbon, that is between the two nitrogen atoms of the imidazolium ring, is the most electron deficient atom in the 1,3- substituted imidazolium cation [23]. Lane G.H. [24] reviewed three possible breakdown methods for 1,3-dialkylimidazoliums. First is a two step reaction, where the initial reaction is to form a neutral radical, and then the radial converts to carbene with hydrogen elimination. The second mechanism is when the two radicals couple to form a dimer. The third reaction is a disproportionation. One radical receives a hydrogen atom to form a simple heterocycle. The other radical converts to a y-lid type structure.

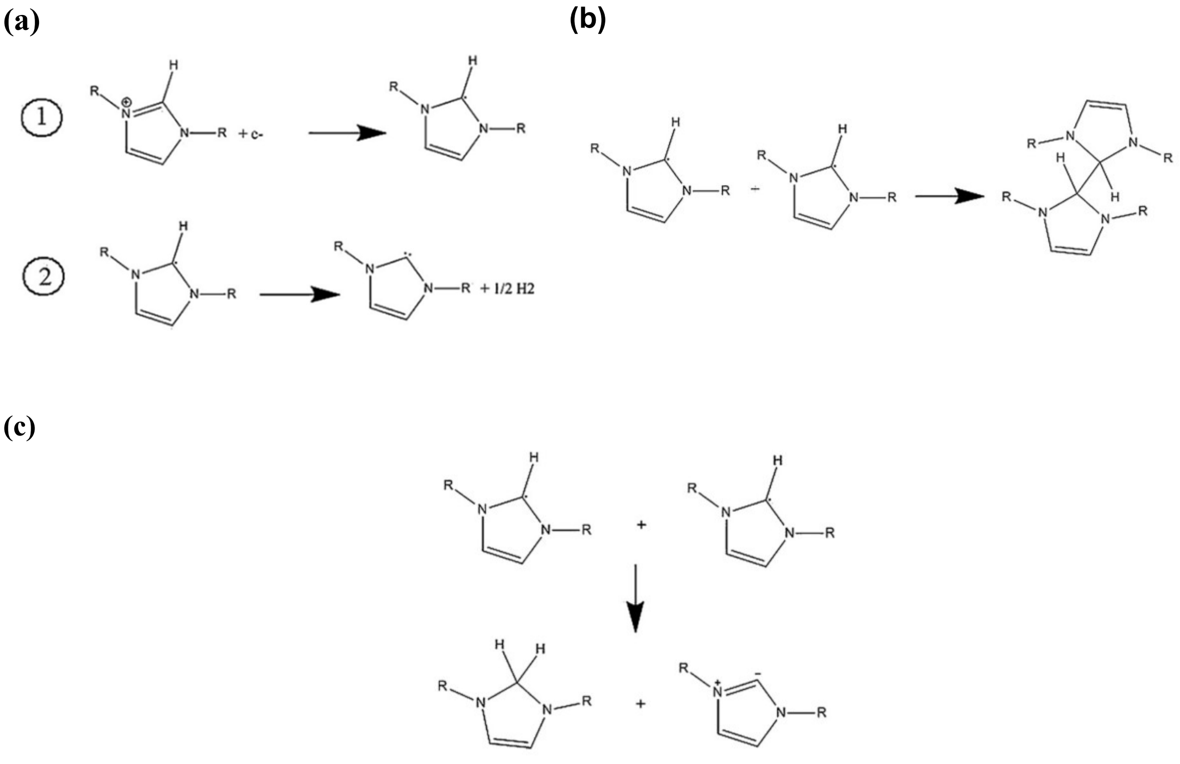

Figure 1.2: Three possible breakdown methods for 1,3-dialkylimidazoliums as proposed from Lane et all,2012. a) The initial reaction is to form a neutral radical, and then the radial converts to carbene b) The two radicals couple to form a dimer.c) Disproportionation, one radical receives a hydrogen atom to form a simple heterocycle. The other radical converts to a y-lid type structure [24].

1.2 Electrochemistry of Lanthanides

The lanthanides series of chemical elements comprises the fifteen metallic chemical elements from lanthanum through lutetium. Common characteristics of lanthanides come from their 4f orbitals, which give lanthanides their acidic behavior, and electrostatic bonding. Lanthanides also have interesting optical properties, such as luminescence for t-t transistors, characteristic emissions for each ion, narrow emission band and long excited lifetimes. Because of their notable properties they are used in a variety of fields and applications, such as catalysts, photoelectrics, optoelectronics, batteries, and nuclear cladding.

1.2.1 Thermodynamics and Half Cell Reactions of Lanthanide Electrochemistry

In electrochemistry, chemical reactions involve the movement of electrons where one chemical reaction gives up electrons (oxidation), and another reaction receives the electrons (reduction). These "redox" reactions are fundamental for all electrochemical disciplines. To illustrate this principle, consider the oxidation half-reaction below in Equation 1.2.

$$\mathrm{Ox} + \mathrm{ne}^- \rightleftarrows \mathrm{Red} \quad \text{(Eqn. 1.2)}$$

Calculations can be used to determine the concentration of free metal ions and the redox potential of the reaction. The electrode half-cell potential of the redox couple can be defined by the Nernst equation given in equation 1.3.

$$\mathrm{E(A)} = \mathrm{E}_o + \left(\frac{\mathrm{RT}}{\mathrm{nF}}\right)\ln\left(\frac{\alpha_{red}}{\alpha_{ox}}\right) \quad \text{(Eqn. 1.3)}$$

where E_0 is the standard redox potential for A, R = 8.314 J/mol K is the gas constant, T the absolute temperature in kelvin, n the number of electrons exchanged, F = 96845 A s/mol is the Faraday constant, and α the activity of the ion [25]. The absolute value cannot be experimentally measured; therefore, the potential is determined as the reduction potential relative to the standard hydrogen electrode, which by definition is zero. A metal can be electrodeposited from solution when the potential applied to the working electrode is more negative than the standard potential E. The driving force for film formation or overpotential is the deviation from equilibrium:

$$\eta = E_{app} - E(A) \quad \text{(Eqn. 1.4)}$$

The metal electrodeposition may occur only when the overvoltage is negative. In contrast, a metal in solution is oxidized (it may dissolve in solution, or form an oxide) if the voltage applied is more positive than E(A). In most practical electrodeposition processes; however, a metal A is reduced from An^+ on a foreign substrate, and an equilibrium for this system cannot be defined rigorously unless the system is left to spontaneously achieve its own equilibrium. In some instances, this equilibrium could be reached quickly with highly reactive metal substrates; in other cases though, the approach to equilibrium can be sluggish. In this case an onset or nucleation overpotential can be defined, as the point which deposition starts to occur.

Presented in equation 1.5 is the reduction of trivalent lanthanum to metallic lanthanum. In order to generate metallic lanthanum out of solution, a more cathodic electrochemical potential than the standard reduction potential must be applied. Table 1.1 below, the electromotive force series, demonstrates that the potential applied must be more negative than -2.4 V vs SHE in order to deposit metallic lanthanum from aqueous solutions.

$$La^{3+} + 3e^{-} \leftrightarrows La^{0} \quad \text{(Eqn. 1.5)}$$

The Table 1.1 below shows standard reduction potentials in decreasing order. The species at the top have a greater likelihood of being reduced, while the ones at the bottom have a greater likelihood of being oxidized. Therefore, when a species at the top is coupled with a species at the bottom, the one at the top will become reduced while the one at the bottom will become oxidized. The standard cell potential of water is between 0 and - 0.828 V vs SHE whereas lanthanides standard cell potentials are around -2.4 V vs SHE. This indicates that electrodeposition of lanthanum from aqueous solutions is impractical because hydrogen will always be present in aqueous solutions and the generation of hydrogen gas from water should always occur before lanthanum deposition can begin to occur. This demonstrates the need for non-aqueous solvent with a large electrochemical window, such as molten salts or room temperature ionic liquids.

Table 1.1: Typical Reduction Potentials in Comparison to the Standard Reduction Potential of Lanthanum.

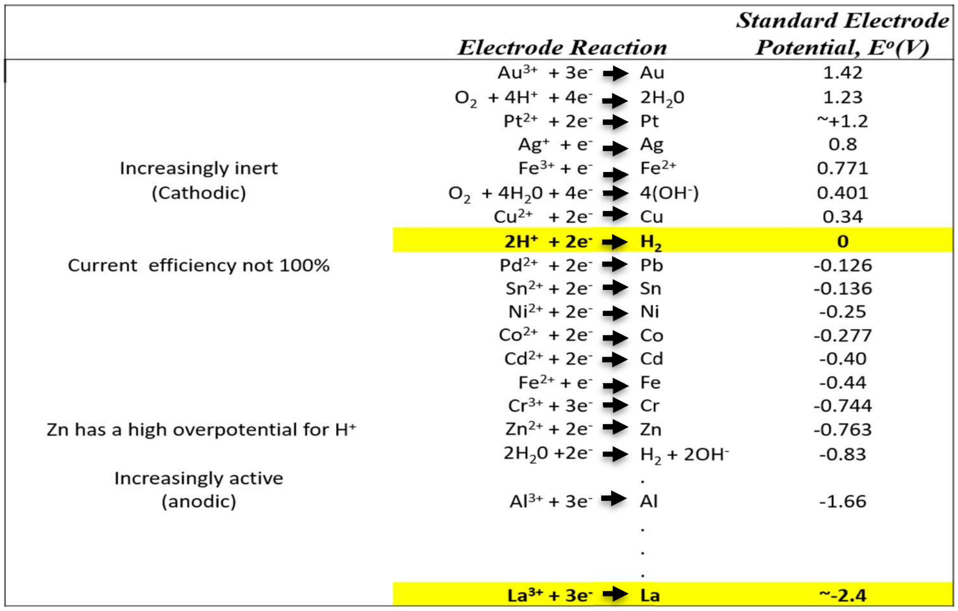

	Electrode Reaction	*Standard Electrode Potential, E°(V)*
	$Au^{3+} + 3e^- \rightarrow Au$	1.42
	$O_2 + 4H^+ + 4e^- \rightarrow 2H_20$	1.23
	$Pt^{2+} + 2e^- \rightarrow Pt$	~+1.2
	$Ag^+ + e^- \rightarrow Ag$	0.8
Increasingly inert	$Fe^{3+} + e^- \rightarrow Fe^{2+}$	0.771
(Cathodic)	$O_2 + 4H_20 + 4e^- \rightarrow 4(OH^-)$	0.401
	$Cu^{2+} + 2e^- \rightarrow Cu$	0.34
	$2H^+ + 2e^- \rightarrow H_2$	**0**
Current efficiency not 100%	$Pd^{2+} + 2e^- \rightarrow Pb$	-0.126
	$Sn^{2+} + 2e^- \rightarrow Sn$	-0.136
	$Ni^{2+} + 2e^- \rightarrow Ni$	-0.25
	$Co^{2+} + 2e^- \rightarrow Co$	-0.277
	$Cd^{2+} + 2e^- \rightarrow Cd$	-0.40
	$Fe^{2+} + e^- \rightarrow Fe$	-0.44
	$Cr^{3+} + 3e^- \rightarrow Cr$	-0.744
Zn has a high overpotential for H⁺	$Zn^{2+} + 2e^- \rightarrow Zn$	-0.763
	$2H_20 + 2e^- \rightarrow H_2 + 2OH^-$	-0.83
Increasingly active	.	
(anodic)	$Al^{3+} + 3e^- \rightarrow Al$	-1.66
	.	
	.	
	.	
	$La^{3+} + 3e^- \rightarrow La$	**~-2.4**

1.2.2 Electrodeposition of Lanthanides from Ionic Liquids

The electrodeposition of lanthanides is commonly performed in high temperature molten salts or organic solvents, due to their high reactivity. While molten salts and organic solvents perform well, they have many economic and environmental problems. Molten salts are highly corrosive and not very cost efficient due to their high temperature operation. While organic solvents can be run at room temperature, they are very volatile to the environment. RTILs have been considered as an alternative to both organic solvents and molten salts because of their properties, including wide electrochemical potential windows, high chemical stability, high ionic conductivity, and their high solubility of metallic salts. Ionic liquids are composed of organic cations and inorganic or organic anions with a large amount of covalent bonding. These liquids can act as a media for chemical and electrochemical reactions because of their high ionic concentration.

The electrodeposition of lanthanides, such as (Nd, Dy, Eu, Yb and Sm) and rare earths, have been performed from various ionic liquids. Researchers primarily used neutral ionic liquids with anions such as Bis(trifluromethylsulfonyl)inde (TFSI). Matsimya et al., [26] electrodeposited Nd from [DEME][TFSI] and determined that the potential influenced the nucleation and growth mechanism. The electrochemical behavior of Ce(IV) in ionic liquid with and without ethanol was studied by Sengupta et al., [27] which showed the nature of Ce from IL and ethanol mixtures. Most of these studies were performed to demonstrate that Ln metals could be electrodeposited from ILs, but some studies on Ln electrochemistry have been performed with rotating disk electrodes. The electrochemistry and coordination Ln^{3+} (Sm, Eu, and Yb) was examined by Hussey and Pan., [28] and Hussey and Chou., [29] later studied the electrochemistry and coordination on Nd and Pr with rotating disk studies. However, their work was primarily focused on electronic absorption not on their RDE studies. Both articles used TFSI with TODGA and chloride for their ionic liquids. Their results determine that only Ln^{3+} ions were produced from these ionic liquids.

1.2.3 Electrochemical Behavior of Lanthanum in Ionic Liquids

The electrodeposition of lanthanum has been studied in both neutral and acidic ionic liquids, but more research is needed. Lageai et al., [30] performed the electrochemistry of La in (OMP-TFSI) with $La(NO_3)$ as a source of lanthanum. Lageai et al., [30] demonstrated that lanthanum could be electrodeposited in ionic liquids. Later, Bourbos et al., [31] proved that the reduction of lanthanum was possible in BMP-TFSI and Me_3NBu-TFSI ionic liquids at room temperature. They also demonstrated that lanthanum electrodeposited from BMP-TFSI was dispersed all over the electrode surface, but when Me_3NBu-TFSI as the ionic liquid, it was mainly observed on the edges of the electrode. To take advantage of the properties of DCA ionic liquids, (BMIM-DCA) ionic liquid were used by Yang et al., [32] to electrochemically prepare lanthanum from $LaCl_3$ as its source. They developed a simple route for the preparation. Using cyclic voltammetry and chronoamperometry they also showed potential influenced the morphology and deposition of lanthanum. These studies did not utilize rotating disk methods and they do not contain key information on lanthanum electrodeposition. The electrochemistry of lanthanum in ionic liquids has not been previously studied with rotating disk methods.

CHAPTER 2: ELECTROCHEMICAL TECHNIQUES

The electrochemical techniques employed in this investigation included the following: controlled cyclic voltammetry (CV), chronoamperometry (CA), and rotating disk electrode voltammetry (RDEV). A brief discussion of each of these techniques appears below.

2.1 Cyclic and Linear Sweep Voltammetry

Cyclic voltammetry is a versatile electrochemical technique that allows one to probe information about a reaction, such as the presence of intermediates, reversibility, electron stoichiometry, diffusion coefficient of analyte and reduction potential [25]. This is accomplished with a three electrode arrangement whereby the potential relative to some reference electrode is scanned at a working electrode while the resulting current flowing through a counter electrode is monitored in an electrolyte. The technique is suited for a quick search of redox couples present in a system. Once located, a couple may be characterized by more careful analysis of the cyclic voltammogram.

CV is a potentiodynamic test that applies current in a linear sweep from an initial potential to a vertex potential. The CV scan generates an oxidized species during the forward scan to potential, then performs a reverse scan that probes the oxidation species. This allows one to study the redox couple of a system. The data is then presented in a current vs. potential graph, which is interpreted to produce information on the thermodynamic and kinetics of the reaction being studied. The important parameters of a cyclic voltammogram are the magnitudes of the anodic and cathodic peak currents potentials shown in Figure 2.1.

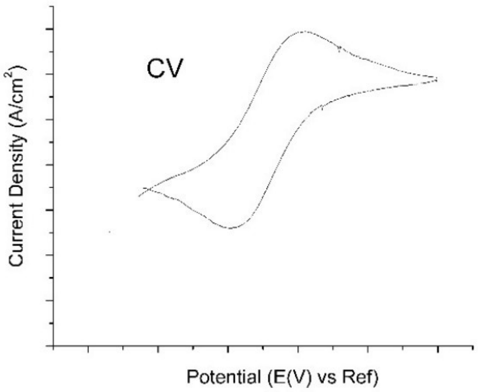

Figure 2.1: CV analysis of a reversible species, where in the cathodic and anodic peaks are symmetric.

The most important information obtained from CV is the reversibility of the redox reactions. An "electrochemically reversible couple" refers to a redox process in which both the oxidized and reduced form of the analyte rapidly exchange electrons at the electrode. The cyclic voltammogram above in Figure 2.1 shows the result of a CV analysis of such a species, wherein the cathodic and anodic peaks are symmetric, but occur at slightly offset potentials. A reversible diffusion controlled reaction is controlled by two laws, the Nernst equation and Flicks law of diffusion. In this case, diffusion limits the reactions and the reaction occurs rapidly so that the reactants can’t reach the electrode. Using Laplace transforms, Nevisian boundary conditions and integration, the peak current is given by Randles-Sevcik equation:

$$i_p = (2.69\times10^5)\, n^{3/2} A D^{1/2} C_o \nu^{1/2} \quad \text{(Eqn. 2.1)}$$

Where n is the number of electrons, A is electrode area, D is the diffusion coefficient, C is the concentration, and ν is the scan rate (V/s). Thus, a great deal of information can be learned about the system by varying known parameters, such as concentration and scan rate.

In case of a irreversible electrode reaction, the rate of electron transfer is insufficient to maintain the Nernstian equilibrium. The shape of CV in that case is different from that for a reversible system. Figure 2.2 located below shows an example of an reversible, quasi-reversible, and irreversible system. Note that in a reversible system peak separation is small, and for an irreversible system, the peak separation becomes more noticeable and father apart. In a case of totally irreversible reaction, the reverse peak is absent.

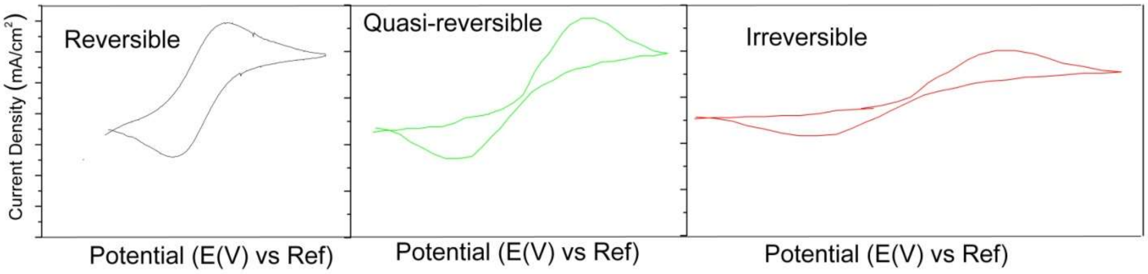

Figure 2.2: Example of a cyclic voltammogram of an reversible, quasi-reversible, and irreversible system.

Linear sweep voltammetry (LSV) is a potentiodynamic technique that scans at a constant rate in one direction the applied potential from an initial potential to a final potential. This technique is technically half a CV scan . Figure 2.3 demonstrates the current density response as the potential is scanned into the cathodic direction. There is no return scan performed in LSV, which makes them useful for imaging the electrode surface without altering the surface with oxidation.

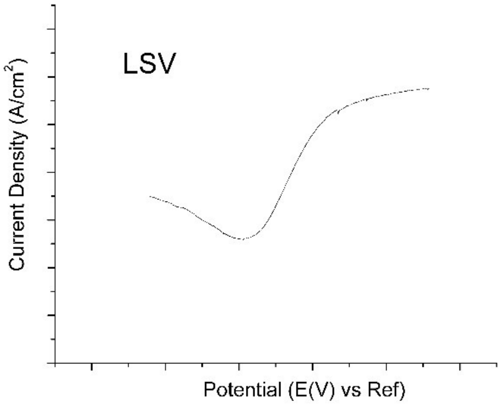

Figure 2.3: Representative LSV plot resulting current density vs applied potential.

2.2 Chronoamperometry

In chronoamperometry, the electrode potential is abruptly changed from E1 (the equilibrium state at this potential) to E2, and the resulting current variation is recorded as a function of time. The interpretation of the results is typically based on a planar electrode in a stagnant solution and an extremely fast interfacial redox reaction as compared to mass transfer [33].

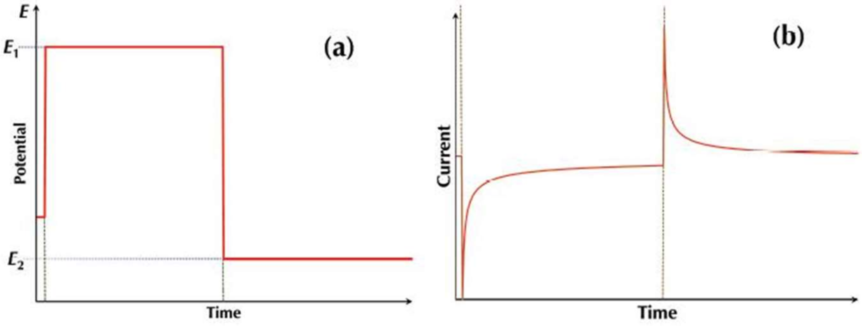

Figure 2.4: a) Potential versus time waveform of chronoamperogram, and (b) resulting current versus time response [33].

The Faradaic current under diffusion controlled conditions is related directly to the concentration gradient, $\partial Ci / \partial x$, evaluated at $x = 0$. Thus, as the slope of the concentration profile for oxidation Ox decreases with time following the potential step, so will the observed current. In the example above, the concentration of Ox at the surface was driven immediately to zero for a step to a potential well negative of the E_0 for the couple. For a reversible system, the ratio of [Red] to [Ox] at the surface is given by the Nernst equation at any potential (see equation 1.3).

Chronoamperometry experiments are most commonly either a single potential step, in which only the current resulting from the forward step as described above is recorded, or a double potential step in which the potential is returned to a final value (Ef) following a time period, usually designated as τ, at the step potential (Es). The most useful equation for chronoamperometry is the Cottrell equation, which describes the observed current (working electrode) at any time following a large forward potential step in a reversible redox reaction (or to large overpotential) as a function of $t^{-1/2}$.

$$I_p = \frac{nFA\ \ ^{1/2}C_o}{\pi^{1/2}t^{1/2}} \quad \text{(Eqn. 2.2)}$$

where n = stoichiometric number of electrons involved in the reaction; F = Faraday's constant, A = electrode area (cm^2), C_0 = concentration of electroactive species (mol/cm^3), and D_0 = diffusion constant for electroactive species (cm^2 /s) [25].

Chronoamperometry lends itself well to the accurate measurement of electrode area (A) by the use of a well-defined redox couple (known n, Co]. With a known electrode area, measurement of either n or D_0 for an electroactive species is easily accomplished by a Cottrell plot. The double potential step method is often applied in the measurement of rate constants for chemical reactions (including product adsorption) occurring following the forward potential step.

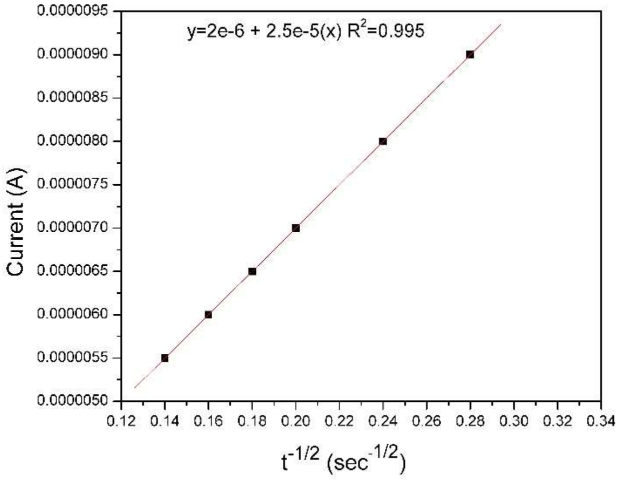

Figure 2.5: Example of a Cottrell plot used for measurement of either n or D_0 for an electroactive species [32].

2.3 Rotating Disk Technique

Rotating disk electrode voltammetry (RDEV) is a useful technique for the study of mass transport and heterogeneous kinetics in an electrochemical system. An important advantage of the RDEV technique is that measurements are made under non-steady-state (i.e., time-independent) conditions [34]. The working electrode commonly consists of a disk of the electrode material, such as a platinum embedded in ceramic sieve. During RDEV experiments, the working electrode is rotated at a constant angular velocity or frequency, ω. The potential is then scanned from an initial value to a final value with a sufficiently slow scan rate to get steady-state currents at the disk electrode.

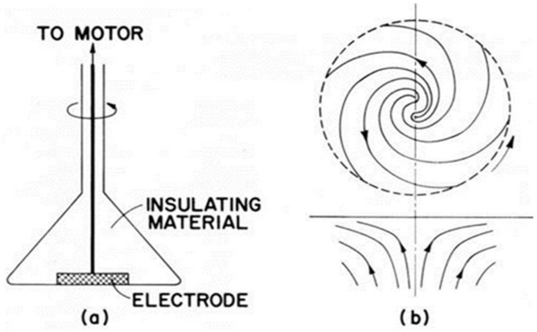

Figure 2.6: Rotating disc electrode; (a) cross section, (b) side and bottom view of liquid flow pattern, from Bockris and Drazic [35].

RDEV at a uniformly accessible disk electrode is probably the most reliable method to study mass transport in solutions because it is based on Levich equation, which is a precise mathematical solution to the convective mass transport equation. In addition, when properly executed, this technique is free from the complications due to uncompensated solution resistance and double layer charging that can affect potential sweep and some potential step techniques. For a reversible chemically stable system, the voltammogram usually has a sigmoidal curve.

The steady state limiting current, iL, can be observed when the electrode process is occurring at the maximum rate possible for a given set of mass-transfer conditions [35]. The diffusion coefficient, D, of reduced or oxidized species can then be calculated by using the Levich equation.

$$|I_L| = -0.620nFAD^{2/3}\ \nu^{-1/6}\, Co\, \omega^{1/2} \quad \text{(Eqn. 2.3)}$$

where A is the electrode area (cm^2), ω is the electrode rotation rate (rad s^{-1}),ν is the kinematic viscosity (cm^2 s^{-1}), and Co represents the bulk concentration of either reduced or oxidized species (mol cm^{-3}), and all other symbols have their usual meaning [34].

Studies based on the Levich equation are a common experiment performed using a rotating disk electrode in which a series of voltammograms are acquired over a range of different rotation rates. For a simple electrochemical system where the rate of half reaction is governed by mass transport, the overall magnitude of the voltammetry should increase (Figure 2.6). The limiting currents of the study are usually plotted against the square root of the rotation rate in what is called a Levich plot (Figure 2.7). Predicted from the Levich equation, if a reaction is purely mass transferred controlled, the limiting current increases linearly with the square root of rotation rate with a slope (0.620nFAD$^{2/3}$V$^{1/6}$C) and intercept at zero.

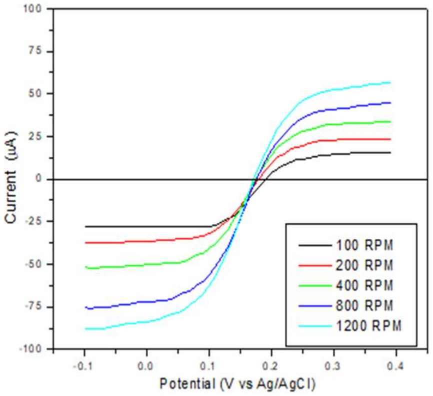

Figure 2.7: A series of voltammograms is acquired over a range of different rotation rates. Limiting currents are the results of being mass transport controlled.

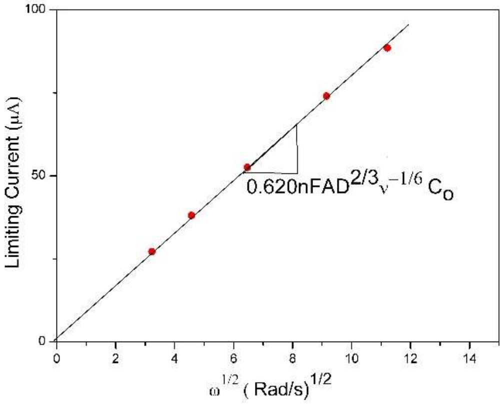

Figure 2.8: Example of a Levich plot for a mass controlled system.

An alternate method of presenting data from a rotating disk studies is based on the rearrangement of the Levich equation in terms of reciprocal current called the Koutecky-Levich.

$$\frac{1}{|I_L|} = \frac{1}{-0.620nFAD^{2/3}\ \nu^{-1/6}\ Co\ \omega^{1/2}} \quad \text{(Eqn. 2.4)}$$

A plot of the reciprocal current versus the reciprocal square root of angular rotation rate (Figure 2.8) can be used to determine the rate constant of a system. For a simple electrochemical reaction (mass transport controlled) the data will fall in a straight line that intercepts zero. If the line intercept is above zero, the reaction is limited by sluggish kinetics characterized with a certain reaction rate constant value (the intercept).

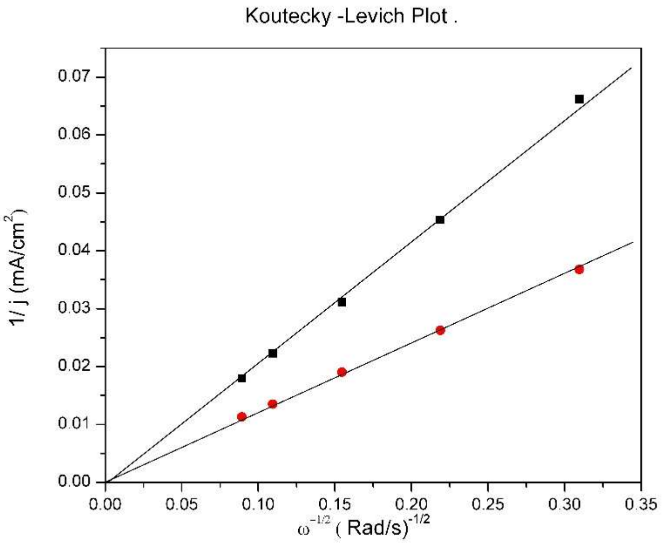

Figure 2.8: Example of a Koutecky-Levich plot for a mass controlled system

CHAPTER 3: EXPERIMENTAL

3.1 Materials

The ionic liquid used was EMIM-DCA produced by Merck, which is no longer in the business of making ionic liquids. The electrolyte was modified to contain 0.1M $LaCl_3$ by first dissolving 0.12260 g $LaCl_3$ in 1.0 g ethanol or water. Before dissolution by hand shaking, mineral sieves were mixed in with ethanol for a minimum of 48 hours to remove all excess moisture. 5 ml of EMIM-DCA was transferred into the same vial with dissolved $LaCl_3$ so that there were no transfer losses. The ionic liquid was then stirred and gently heated in a furnace designed for molten salt experimentation at 80 C until the solvent was evaporated. A vacuum was provided by an external diaphragm pump connected to the vial capped with a Leuer lock with tygon tubing. The weight of the solution was used as a diagnostic. If the weight was stable, the solvent was evaporated. EMIM-DCA with and without $LaCl_3$ was also measured with additional ethanol to determine if ethanol had an the electrochemistry of lanthanum and or EMIM-DCA.

3.2 Glove Globe

A glove globe very similar to a glove box was designed by Dr. Batric Pesic [36] to perform electrochemical studies in closed atmosphere. The glove globe was maintained at low ppm of moisture during each experiment of this research. It was filled three times with ultra-high purity argon gas (99.999% pure) before each experiment. A threat to the validity of any of the experimental work carried out in the glove globe is very low or nonexistent. The glove globe was designed with two small transfer chambers on the top to allow the transfer of the working electrode, reference electrode and electrochemical cell between experiments. The vacuum pressure was controlled manually with a mechanical pump. Once the desired vacuum level was achieved, the valves closed and the vacuum pump was turned off.

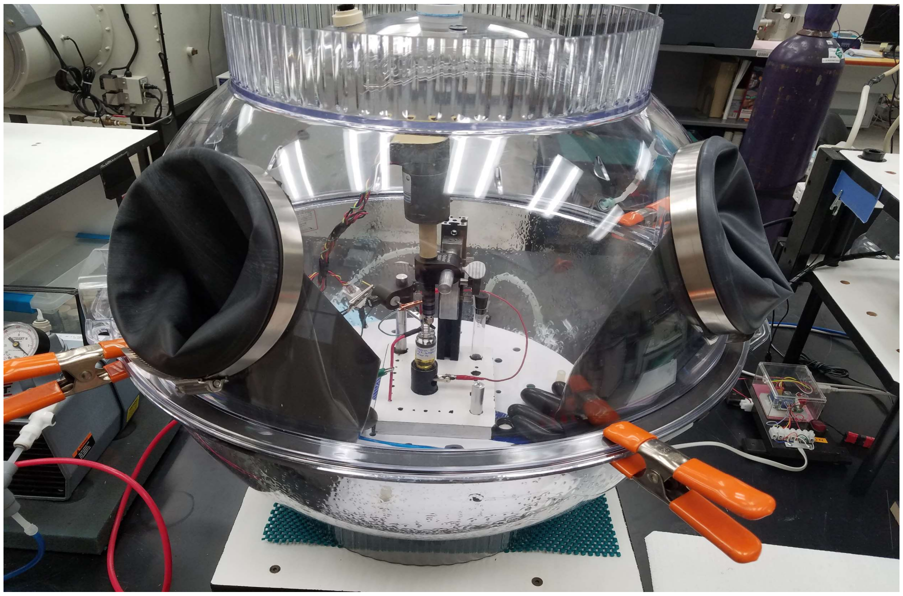

Figure 3.1: Glove globe with rotating disk setup used for closed atmosphere electrochemical studies [36].

3.3 Electrochemical Cell

Electrochemical experiments were carried out with a three-electrode cell designed by Dr. Batric Pesic,.[36] shown in Figure 3.2. The electrochemical cell was made with two vials attached with epoxy. The bottom of the cell contained a graphite counter electrode (CE) about a (6 mm diameter) surrounded with teflon to prevent leaking. The top of the cell was left open for the leak free Ag/AgCl reference electrode (RE) and the Pt90Ir10 rotating working electrode (WE). The Pt90Ir10 electrode (2.35 mm diameter) was prepared by polishing with a 0.5 μm Al_2O_3 solution on a pad, rinsed and sonicated with DI water, and dried with a hand drier before each experiment. To perform electrochemical experiments in ionic liquids, a reliable reference electrode is needed. For each ionic liquid system and operating temperature, a reference electrode must be carefully chosen to operate reliably under the appropriate measurement conditions. [37] For this study, the reference electrode used was a leak free Ag/AgCl. This reference electrode is not normally used in ionic liquids, but in EMIM-DCA it was stable. Before each experimental set, the reference electrode was measured against a master electrode.

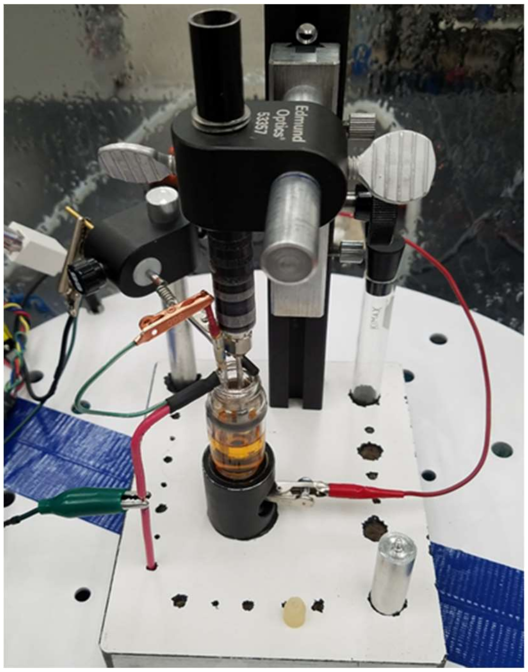

Figure 3.2: Electrochemical cell for studies of lanthanum from EMIM-DCA-LaCl3 ionic liquid. Working electrode is Pt90Ir10 (2.34 mm dia), reference is a leak free Ag/AgCl electrode, and counter electrode is a 6 mm dia graphite disk [36].

3.4 Rotating Disk Setup

Lanthanum electrodeposition was studied using the rotating disk technique inside and outside a glove globe. The rotator used was specially designed to work in and outside the glove globe/box by Pesic [36]. It was transferred into the glove globe in dismantled form and assembled in the glove globe. The rotator consists of: a vertical optical mount bar with a moving stage, a glued PVC tube for the accommodation of an electrode cell and clamping of a counter electrode through a hole on the side of the tube, Pittman DC Motor, and Dremel shaft for accommodating the working electrode. The speed of rotation was controlled by EZCommander by AllMotion.

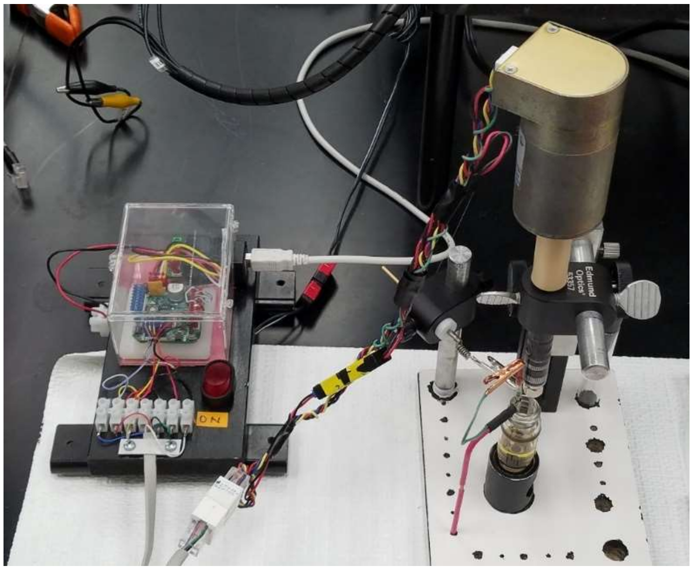

Figure 3.3: Electrochemical setup for rotating disk studies of lanthanum from EMIM-DCA-$LaCl_3$ ionic liquid [36].

3.5 High Temperature Setup

Figure 3.4 presents the experimental setup with a heater added in order to perform experiments to determine the effects of temperature. Notice the heater and the thermocouple lead. This thermocouple was connected to a proportional temperature controller for accurate control of the temperature during experiments.

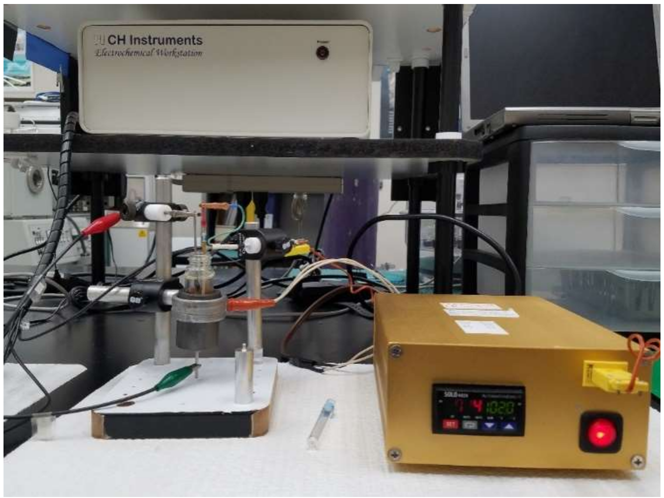

Figure 3.4: Electrochemical setup for high temperature deposition of lanthanum from ionic liquids [36].

CHAPTER 4: RESULTS AND DISCUSSION

This chapter reports and analyzes the data obtained by means of rotating disk and voltammetry. The rotating disk method and its the implementation were introduced in a previous chapter. Rotating disk studies of EMIM-DCA with $LaCl_3$ were studied in an open atmosphere (Sec. 4.1). Open atmosphere studies were compared to closed atmosphere in (Sec. 4.2). The main system investigated in this work was the effect of ethanol and water on EMIM-DCA with and without $LaCl_3$ (Sec. 4.3, Sec 4.4 and Sec 4.5). The morphology of films are in the next chapter.

As a baseline for the studies, the effect of scan range was performed on EMIM-DCA with and without $LaCl_3$ (Figure 4.1). Both plots shown that the reduction of EMIM-DCA on platinum occurs at -1.8 V vs Ag/AgCl. Notice that in the CVs without $LaCl_3$ the currents produced are much more cathodic, since the EMIM+ cation of EMIM-DCA has nothing with which to react.

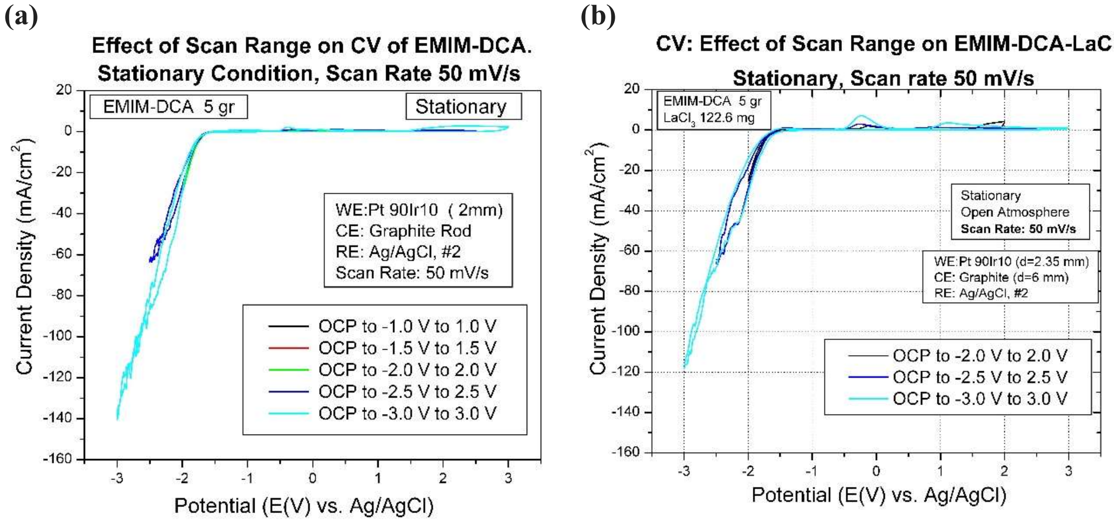

Figure 4.1: Effect of scan range on CV of EMIM-DCA with and without $LaCl_3$ present. (a) EMIM-DCA only (b) EMIM-DCA-$LaCl_3$

4.1 Rotating Disk Studies of $LaCl_3$ in EMIM-DCA

Baseline linear sweep voltammetry (LSV) scans of EMIM-DCA containing lanthanum chloride in open atmosphere are shown below in Figure 4.2 a-b.

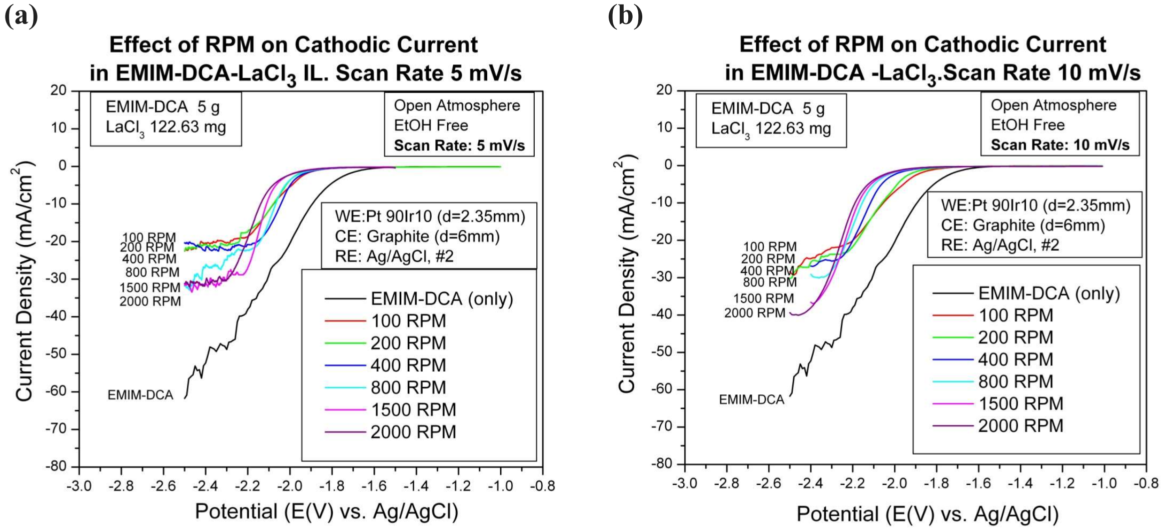

Figure 4.2: LSV of EMIM-DCA with $LaCl_3$ present. Effect of RPM and scan rate on the electrodeposition of La (a) 5mV/s (b) 10 mV/s.

The voltammograms in Figure 4.2 show EMIM-DCA with lanthanum chloride at two scan rates and multiple RPMs. The ionic liquid was colored yellow, but was still clear and no particulates were seen. These scans show limiting currents around -2.2V. Bubbles were formed on the working electrode as the potential was scanned cathodically around -1.8 V vs Ag/AgCl from either H_2 or ethane. Lanthanum films were deposited during the LSV scans (Figure 4.2 a, b). Figure 4.3 provides a Levich plot of EMIM-DCA with lanthanum chloride between 100 and 2000 RPM. An intercept is seen in the Levich plot which is consistent with a reaction that has a kinetic controlling parameter. The diffusion coefficients of lanthanum at 10mV/s and 5mV/s in EMIM-DCA were calculated to be $7.6x10^{-7}$ cm^2/sec via the Levich equation. Table 4.1 shows the data used to create the Levich plots.

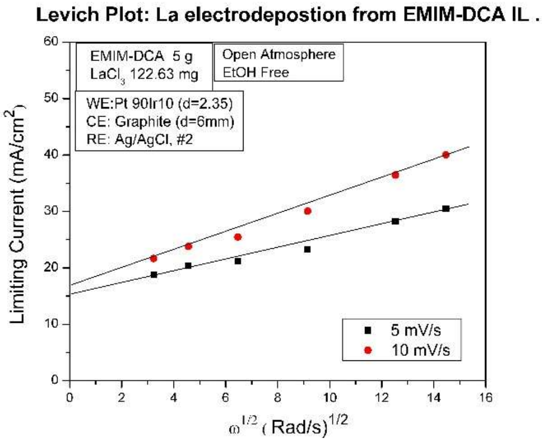

Figure 4.3: Levich plot of EMIM-DCA with LaCl$_3$. Experiment performed in open atmosphere.

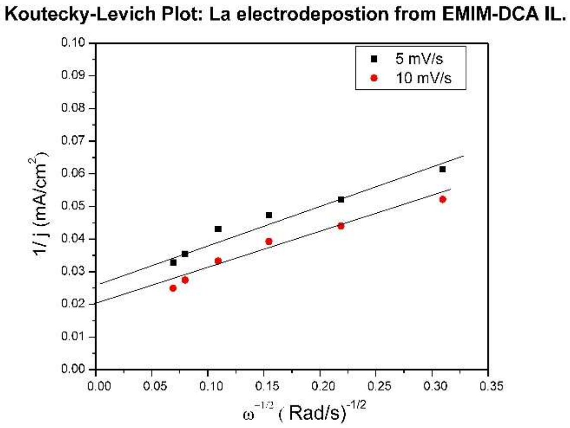

Figure 4.4: Koutecky-Levich plot of EMIM-DCA with LaCl$_3$. Experiment performed in open atmosphere.

Table 4.1: Limiting current values obtained from LSV of EMIM-DCA with LaCl$_3$ under different rotation speeds and scan rates

	Current Density mA/cm^2					
Scan Rate	RPM					
	100	200	400	800	1500	2000
10 mV/s	21.67	23.80	25.47	30.06	36.45	40.05
5 mV/s	18.82	20.37	21.16	23.24	28.19	30.46

Overall ionic liquids have had slow development in studies by rotating disk. Among several concerns such as the higher costs and stability of the solvents, the transport properties of ionic liquids definitely affect the stability of the film [38]. Our system appears to have mixed kinetics which means the reaction is not completely mass transport or reaction controlled. The Levich and Koutecky-Levich plot for EMIM-DCA-LaCl$_3$ appear to be linear at slower scan rates, however both plots have y intercept being located above the origin. This indicates that the deposition of lanthanum from EMIM-DCA is not purely mass transport controlled. One reason as Giaccherini et al, [38] stated is that the velocity field cannot be well developed in ILs, since the dragged layer is comparable with the radius of working electrode. However, EMIM-DCA has the lowest viscosity of any ionic liquid, therefore the dragged layer should be minimized.

4.2 Studies of $LaCl_3$ in EMIM-DCA in Inert Atmosphere

Baseline CV and LSV scans of EMIM-DCA containing lanthanum chloride in inert atmosphere are shown below in Figures 4.5 and 4.6**.**

(a)

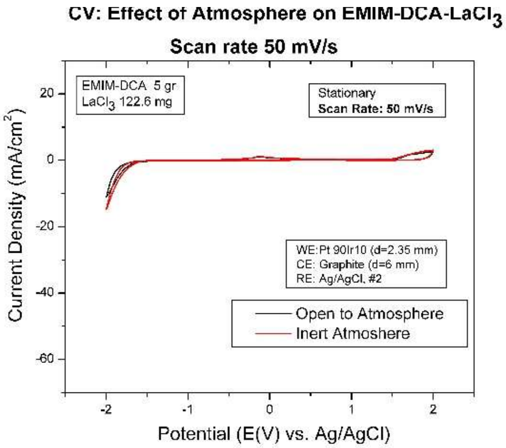

Figure 4.5: CV of EMIM-DCA with $LaCl_3$ present. Inert Atmosphere vs Open to atmosphere.

(b)

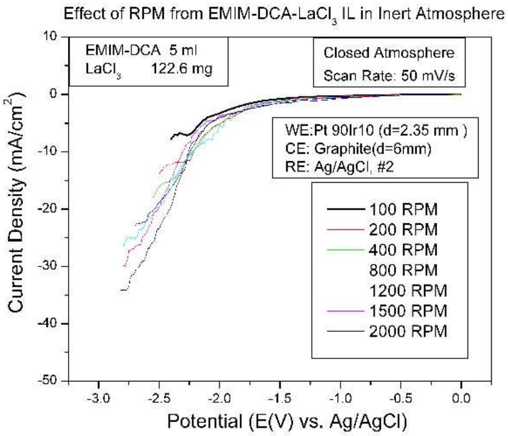

Figure 4.6: Effect of RPM on LSV of EMIM-DCA-$LaCl_3$. Inert Atmosphere.

The voltammograms in Figure 4.5 and 4.6 show EMIM-DCA with lanthanum chloride in inert atmosphere. These scans show no difference from open atmosphere as demonstrated by Figure 4.5. Bubbles were formed on the working electrode as the potential was scanned cathodically around -1.8 V vs $Ag/AgCl_3$. Films were deposited during the LSV and CV scans; no difference was seen therefore all test were run in open atmosphere.

4.3 Effect of Ethanol Addition to EMIM-DCA with and without $LaCl_3$

Since ethanol is a common solvent used to dissolve lanthanum chloride for addition to the ionic liquid, the next work done with ionic liquid was to study the stability of ethanol in the ionic liquid with and without any metal present. CV in EMIM-DCA without lanthanum chloride was performed in the cathodic region to study the reduction behavior of ethanol and the results are shown in Figure 4.7a. Figure 4.7b shows the CV performed to study the effects of ethanol addition to EMIM-DCA with lanthanum chloride. Electrode rotation was studied in order to remove bubble formation on electrodes, however no effect on the electrochemical reaction demonstrated by Figures 4.7 c-d. Figures 4.7a-d show no distinct peaks or limiting currents. Bubbles were formed on the working electrode as the potential was scanned cathodically around -2 V vs Ag/AgCl. This shows that ethanol causes no drastic change compared with pure EMIM-DCA.

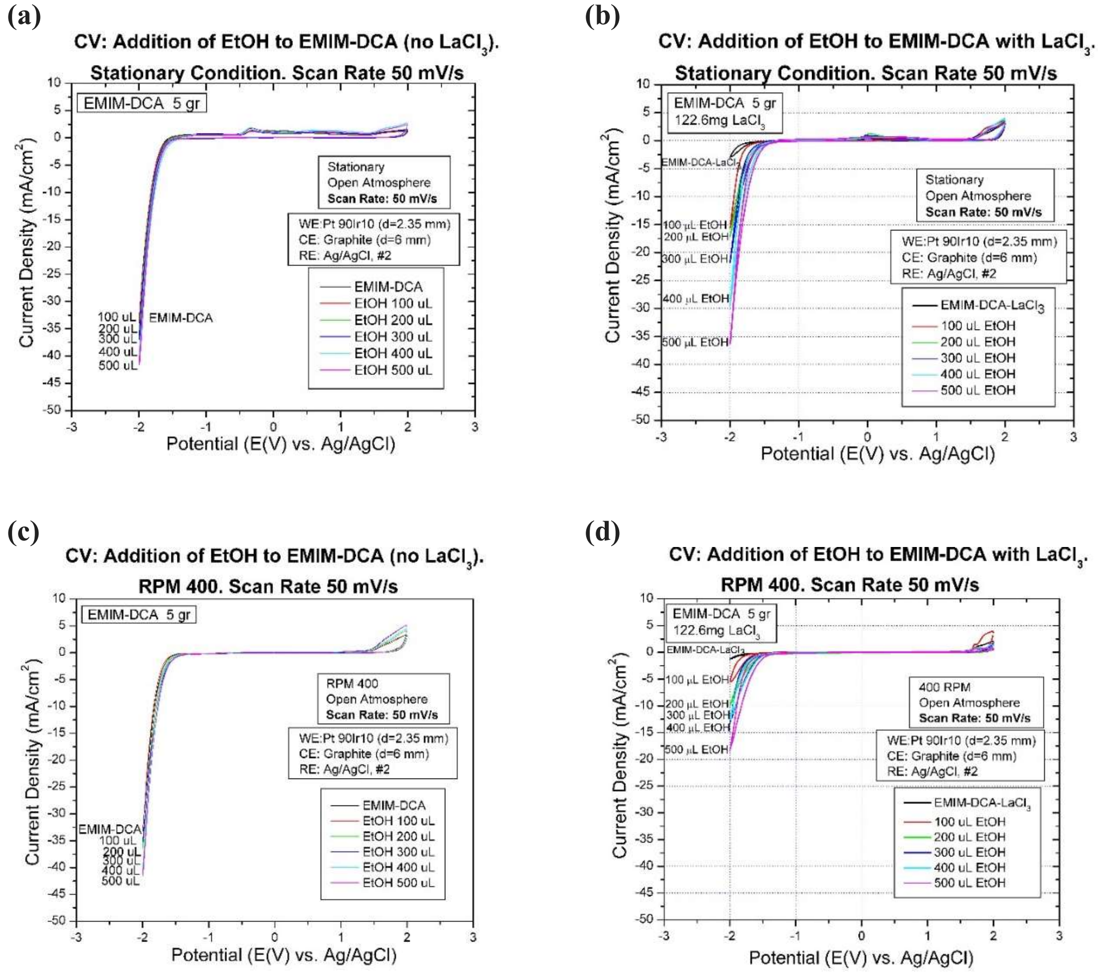

Figure 4.7: Effect of ethanol addition on the CV of EMIM-DCA with and without $LaCl_3$. (a) EMIM-DCA (No $LaCl_3$). (b) EMIM-DCA-$LaCl_3$. LSV performed at 50 mV/s at 0 RPM. (c) EMIM-DCA (No $LaCl_3$). (d) EMIM-DCA-$LaCl_3$. LSV performed at 50 mV/s at 400 RPM.

4.4 Effect of EMIM-DCA Addition to Ethanol with and without $LaCl_3$

In order to further study the ethanol and EMIM-DCA reduction reactions, CVs were performed using 5 mL of ethanol as the electrolyte with incremental additions of ionic liquid to supply conductivity. CVs were performed in the range where ethanol is active, to study the reduction behavior of EMIM-DCA in ethanol. Figures 4.8 a-d show the CVs performed to study the effect of EMIM-DCA addition to ethanol without $LaCl_3$. The CV on effect EMIM-DCA addition to ethanol with $LaCl_3$ at stationary condition is shown in Figure 4.8b. As the concentration of EMIM-DCA rises, an increase is seen in the cathodic currents combined with an anodic shift in the breakdown potential. Three possible reactions are proposed from Schmidt et al., [39] for ethanol reduction; 1) the adsorption of negative charged ethanol radical. 2) The radical can either be reduced to form ethane or methane, or 3) the radical could react with EMIM cation. A consistent increase in currents is seen with increasing ionic liquid concentration with and without lanthanum present.

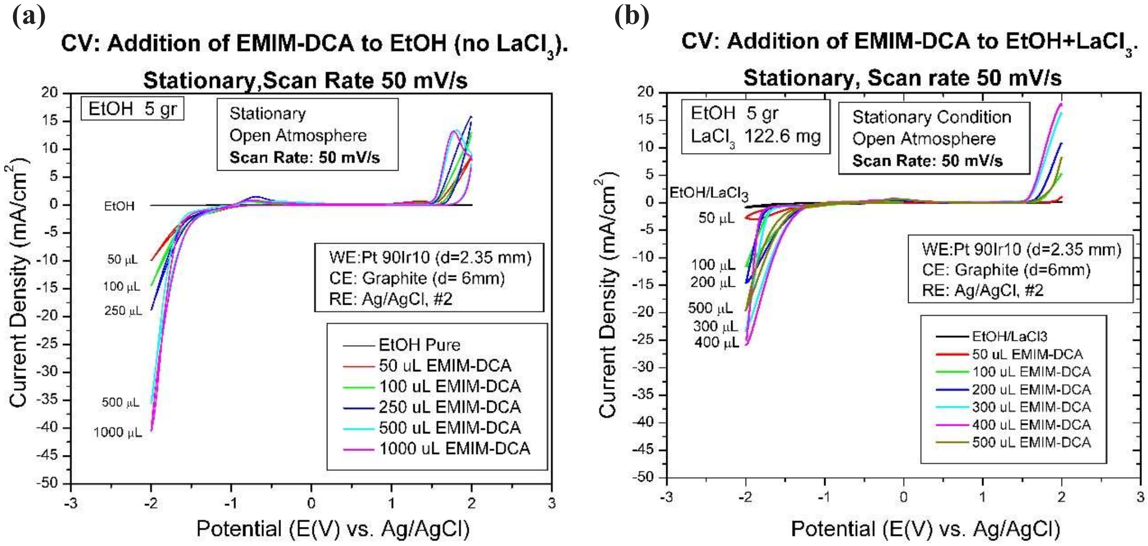

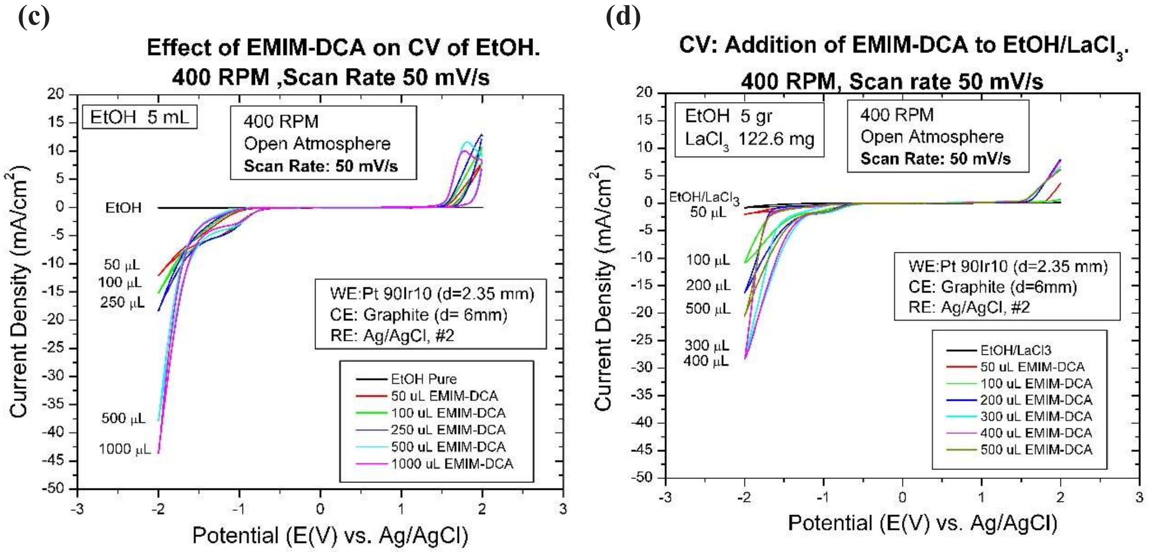

Figure 4.8: Effect of EMIM-DCA addition on the CV of EtOH with and without $LaCl_3$. (a) CV without $LaCl_3$ present, performed at 50 mV/s at 0 RPM. (b) CV with $LaCl_3$ performed at 50 mV/s at 0 RPM. (c) CV without $LaCl_3$ present, performed at 50 mV/s at 400 RPM. (d) CV with $LaCl_3$ performed at 50 mV/s at 400 RPM.

Figures 4.8a-d show CVs performed on the addition of EMIM-DCA to ethanol without and with $LaCl_3$. When a small amount of EMIM-DCA (50 µL) is added to ethanol with $LaCl_3$, EMIM cation film production is observed at a scan range of -2V to 2V. This is interesting since the EMIM cation shouldn't deposit until all ethanol is consumed. Figure 4.8b shows two distinct peaks as a result of the lanthanum morphology. The scans without rotation have larger cathodic currents because the rough film deposit increases the surface area for reaction. With stirring, the EMIM film is smooth and has smaller surface area demonstrated by Figure 4.8d.

4.5 Effect of Water Addition to EMIM-DCA with and without $LaCl_3$

Similar experiments were carried out with water, since water can be absorbed from the atmosphere. Figures 4.9a-d show CVs performed on the addition of H_20 to EMIM-DCA with and without $LaCl_3$, CV of water addition to EMIM-DCA at 0 RPM is shown in Figure 4.9a, and CV of water addition to EMIM-DCA with $LaCl_3$ at 0 RPM is shown in Figure 4.9b. CV of water addition to EMIM-DCA at 400 RPM is shown in Figure 4.9c, and the CV of water addition to EMIM-DCA with

$LaCl_3$ at 400 RPM shown in Figure 4.9d.

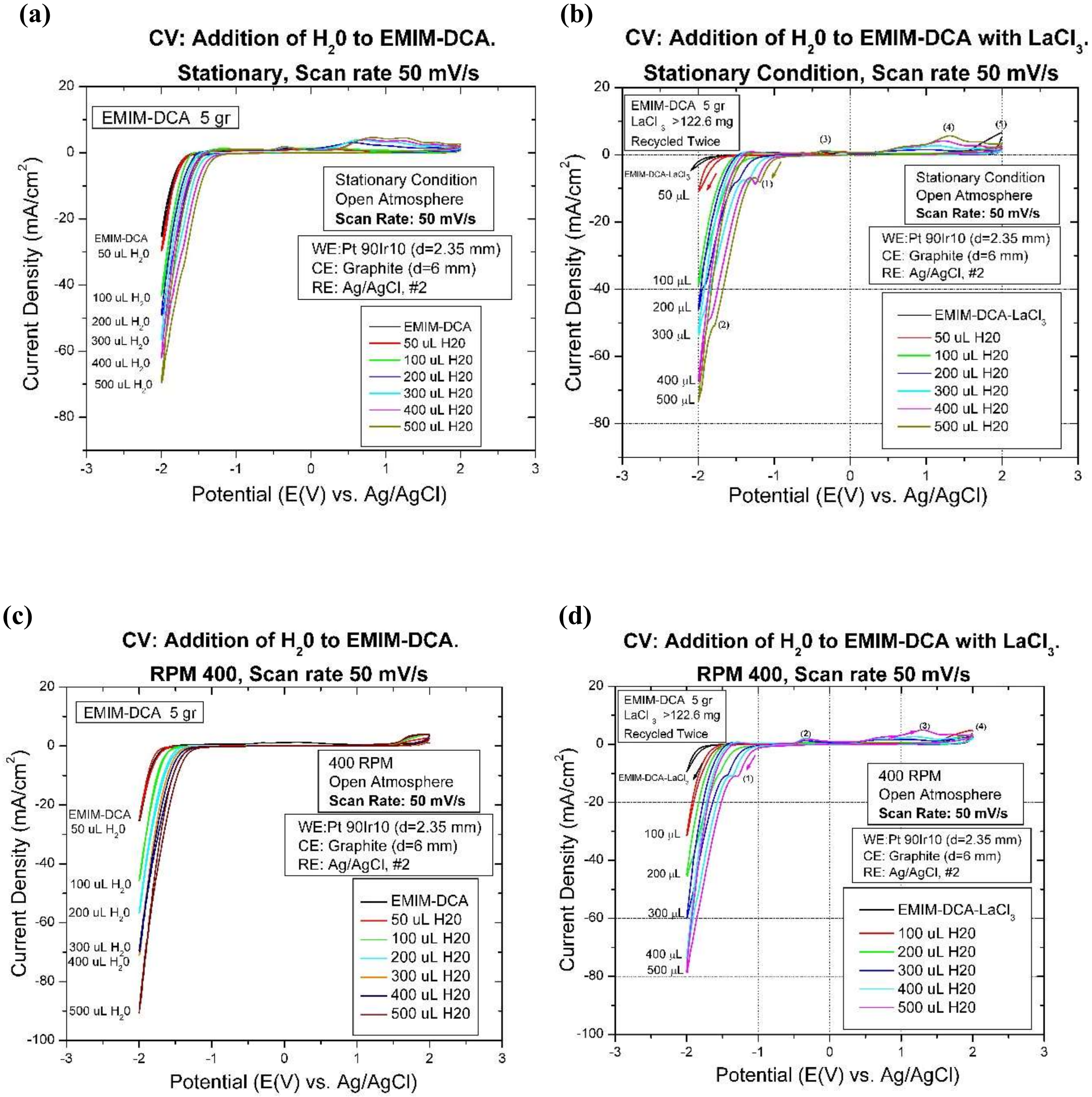

Figure 4.9: Effect of H_20 addition on the CV of EMIM-DCA with and without $LaCl_3$. (a) CV without $LaCl_3$ performed at 50 mV/s at 0 RPM. (b) CV with $LaCl_3$ performed at 50 mV/s at 0 RPM. (c) CV without $LaCl_3$ performed at 50 mV/s at 400 RPM. (d) CV with $LaCl_3$ performed at 50 mV/s at 400 RPM.

CVs were performed in the range where ethanol is active, to study the reduction behavior of EMIM-DCA with moisture. Figure 4.9a shows no distinct peaks or limiting currents and behavior similar to the incremental addition of ethanol to EMIM-DCA. The effect of moisture on the ionic liquid EMIM-DCA therefore is small. Figure 4.9b shows a distinct peak at around -1.25 V after about 300 uL of water is added. Upon looking at the microstructure, a film is made from the reaction between water and the ionic liquid. Note that the current remains the same but the potential at which the reaction occurs is lowered with addition of water.

To further evaluate the reaction between water and EMIM-DCA with LaCl$_3$, Randles Sevcik plots with and without rotation were created to determine the reversibility of the reaction**.** Figures 4.10 a, b show the effect of scan rate on the CV of EMIM-DCA-LaCl$_3$ with 500 uL of water with and without rotation. As scan rate increases the peak potential decreases indicating a irreversible reaction. Values obtained from Figures 4.10 a, b were used to create the Randles Sevcik plots in Figures 4.11 a, b.

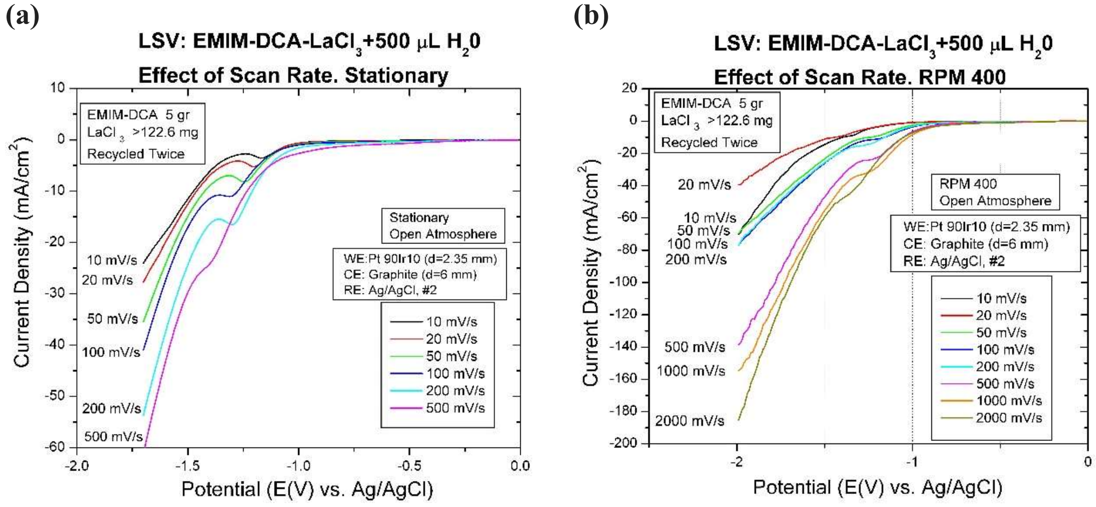

Figure 4.10: Effect of scan rate on EMIM-LaCl$_3$ + 500 uL H$_2$0. (a) LSV performed at 50 mV/s at 0 RPM. (d) CV performed at 50 mV/s at 400 RPM**.**

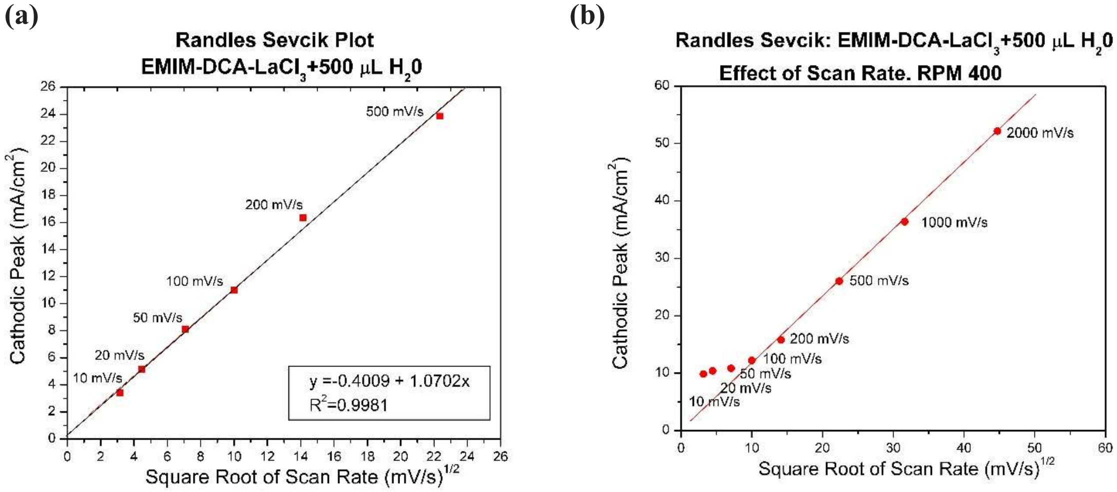

Figure 4.11: Randles Sevcik plot on reaction of EMIM-$LaCl_3$ + 500 uL H_20. (a) CV performed at 50 mV/s at 0 RPM. (d) CV performed at 50 mV/s at 400 RPM.

Films were deposited during the CV scans, the effect of RPM on EMIM-DCA-$LaCl_3$ with water is shown in (Figure 4.12). Figure 4.13 provides a Levich plot of EMIM-DCA-$LaCl_3$ and 500 uL H_20 between 200 and 1500 RPM. Figure 4.14 provides a Koutecky Levich Plot of EMIM-DCA-$LaCl_3$ and 500 uL H_20. An intercept is seen in both the Levich and Koutecky Levich plot which is consistent with a reaction that has reaction controlling parameter similar to the system without water.

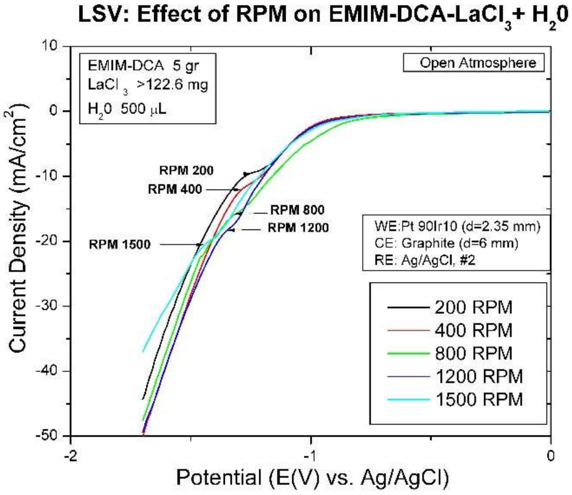

Figure 4.12: LSV of EMIM-DCA- $LaCl_3$ with 500 uL H_20. Effect of RPM on the electrodeposition of water.

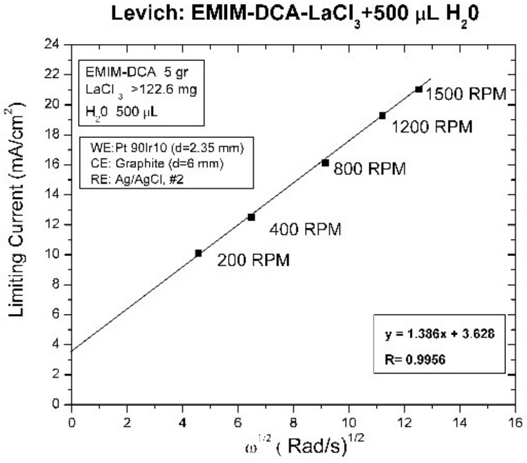

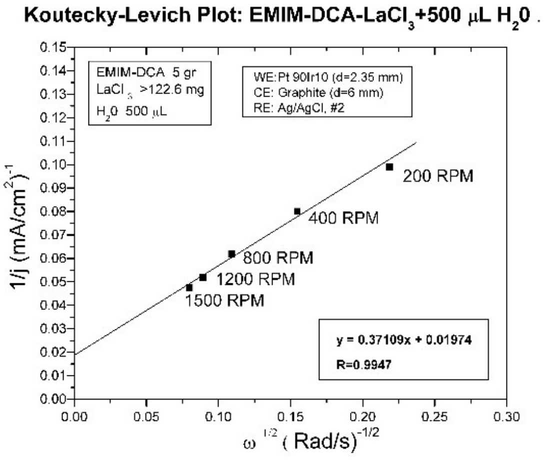

Figure 4.13: Levich plot of EMIM-DCA- $LaCl_3$. with 500 uL H_20.

Figure 4.14: Koutecky-Levich plot of EMIM-DCA-$LaCl_3$ with 500 uL H_20.

The addition of H_20 decreases the viscosity of the EMIM-DCA, but the rotating disk studies of EMIM-DCA with water demonstrated the same features as without. The diffusion coefficient of water in EMIM-DCA were calculated to be $7.6x10^{-7}$ cm^2/sec and $1.8x10^{-9}$ cm^2/sec respectively. The reduction of water on platinum in EMIM-DCA exhibited sluggish kinetics and the rate constant was calculated to be $2.15x10^{-5}$ cm/sec.

4.6 Effect of Electrode Surface on BMIM-DCA with and without $LaCl_3$

The electroactive windows and working potential for morphology were determined for each electrolyte by the following cyclic voltammograms. Different electrodes such as platinum, copper and glassy carbon were used, to analyze the morphology of lanthanum on the different surfaces. Before analyzing the morphology the reduction limit at each electrode needed to be determined. CVs on BMIM-DCA with and without La were measured on three different electrodes (Figure 4.15).

For BMIM-DCA and EMIM-DCA, the reduction limit appeared at about -1.8 V vs. Ag/AgCl on platinum, However on glassy carbon, the reduction potentials is about -2.4 V vs. Ag/AgCl. The reductive limit also seemed to vary slightly towards more positive potentials with an increasing amount of RTIL. The major difference in platinum vs glassy carbon, is their ability to reduce hydrogen. Platinum is a good reducer of hydrogen; therefore bubble formation and cation reduction occurs much earlier on platinum. Glassy carbon on the other hand has an amorphous surface preventing the formation of cation on the electrode surface.

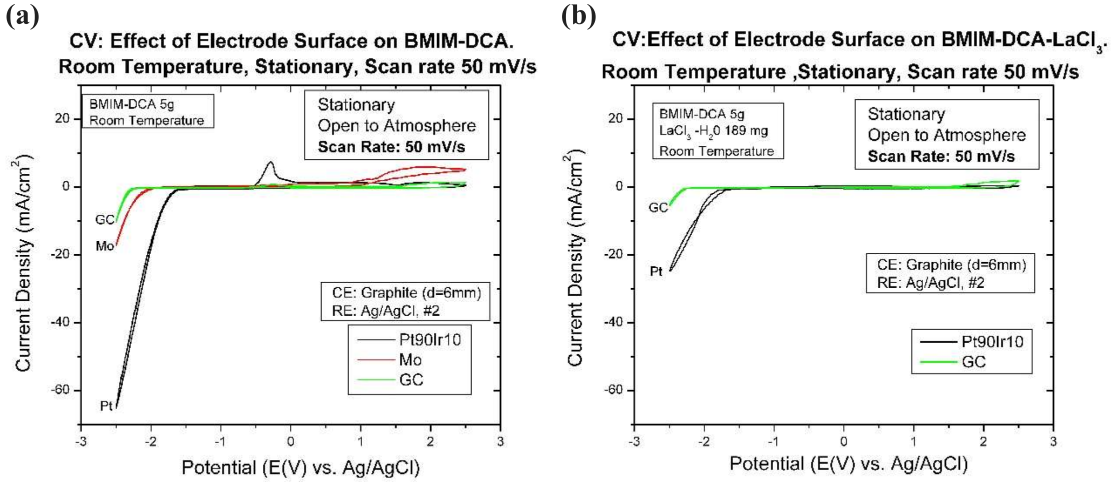

Figure 4.15: Effect of Electrode Surface on the CV of BMIM-DCA with and without $LaCl_3$. (a) CV without $LaCl_3$ performed at 50 mV/s at 0 RPM. (b) CV with $LaCl_3$ performed at 50 mV/s at 0 RPM

CHAPTER 5: SURFACE MORPHOLOGY AND CHARACTERIZATION

5.1 Optical Characterization of Electrodeposited Films on a Pt Working Electrode

For the optical characterization of electrodeposited films on a Pt working electrode, chronoamperometry was used to create the films at various potentials Figure (5.1). The choronamperograms did not show any peaks, however a slight decrease of the current sometimes occurred due to a non-constant bubbling. No peak formation occurred since organic and lanthanum deposition occurred at the same time, therefore Scharifker-Hills model could not be used to determine if the nucleation was instantaneous or progressive.

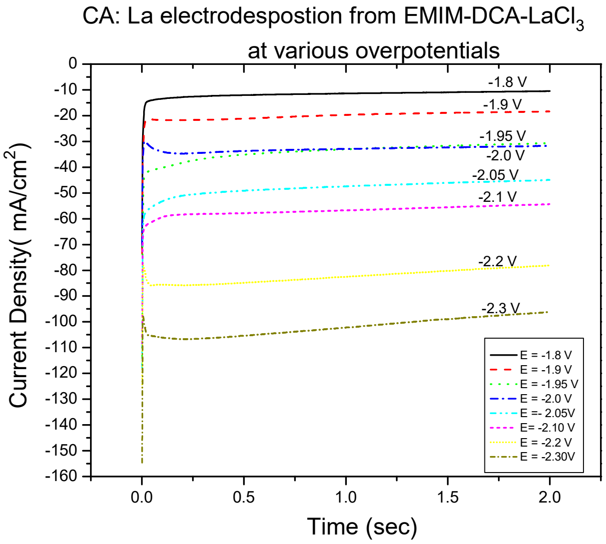

Figure 5.1: Chronoamperometry of EMIM-DCA-LaCl$_3$ at various overpotentials.

Optical microscopy was first used to evaluate the effect of applied potential on the surface morphology of lanthanum formed on platinum electrode, shown by Figures (5.2 a-f) located below. The electrode was cleaned by three methanol washes to remove any organics or ionic liquid from the surface and dried with air before any microscopy. If needed the surface was also cleaned via methanol chloride to remove residual methanol from the surface of the electrode.

(a) -1.7 V EMIM-DCA-LaCl$_3$ (b) -1.8V EMIM-DCA-LaCl$_3$ (c)-2.0V EMIM-DCA-LaCl$_3$

(d) -2.2V EMIM-DCA-LaCl$_3$ (e) -2.4V EMIM-DCA-LaCl$_3$ (f) -3.0V EMIM-DCA-only

Figure 5.2 Optical microscopy of film developed by chronoamperometry performed at room temperature with EMIM-DCA for 3 sec at various potentials. Clean via methanol wash procedure.

Figures 5.2 a-f present optical micrographs at 40x for chronoamperometry performed at room temperature with EMIM-DCA with and without LaCl$_3$. At -1.7 V vs Ag/AgCl, the current of the CA (Figure 5.1) did not decrease but stayed constant zero during the deposition time. This means that no deposition occurs at -1.7 V which was confirmed by the absence of visible deposit on the electrode (Figure 5.2a). These results do not agree well with the information presented in Table 1.1 which postulates that lanthanide deposition should not occur until a potential of -2.4 V is applied at room temperature. In Figures 5.2b and 5.2c a distinct film is seen on the electrode surface with polarization potentials of -1.8 and -2.0 V respectively. These potentials correspond well with the onset of lanthanum deposition beginning to occur at -2.0 V.

At the potential of -2.0 V the formation of bubbles starts to occur intercepting film formation, as seen in Figure 5.2c around the edge of the electrode. The bubbles are explained by the presence of hydrogen from the open atmosphere or the reduction products of EMIM, and BMIM. As discussed above, the cation is proposed to follow a two-step reduction process to carbene via removal of hydrogen, and hydrogen gas is also produced from water. When the potential is increased more than -2.0V in applied over potential more bubbling is present on the electrode surface. Polarization at -2.4 V in Figures 5.2e leads to further bubbling on the electrode surface, completely disrupting the lanthanum film. Figure 5.2f presents the electrode surface after polarization at -3 V for 3 seconds in pure EMIM-DCA with no lanthanum present. The bare surface evident in Figure 5.2f indicates that even up to -3 V, the deposits seen in Figure 5.2 a-g should be attributed to the reduction of lanthanum.This demonstrates that the film is not deposited EMIM cation or an organic compound

5.2 SEM Characterization of Electrodeposited Films

The high temperature setup shown in Figure 5.4 was used to study the film morphology at higher temperature. Figure 5.3a-d below present electron micrographs of the platinum working electrode after CA performed in BMIM-DCA with $LaCl_3$. This electrode was polarized at -2.0 V for 2 hours with the temperature increased to 80° C. The increased temperature prevents BMIM cations from covering the surface of the working electrode allowing more places for lanthanum deposition. The higher temperatures should also increase the mass transfer and conductance of ionic liquid. The temperature also can reduced the amount of hydrogen absorb from the atmosphere by the ionic liquid as well as remove impurities already in the ionic liquid.

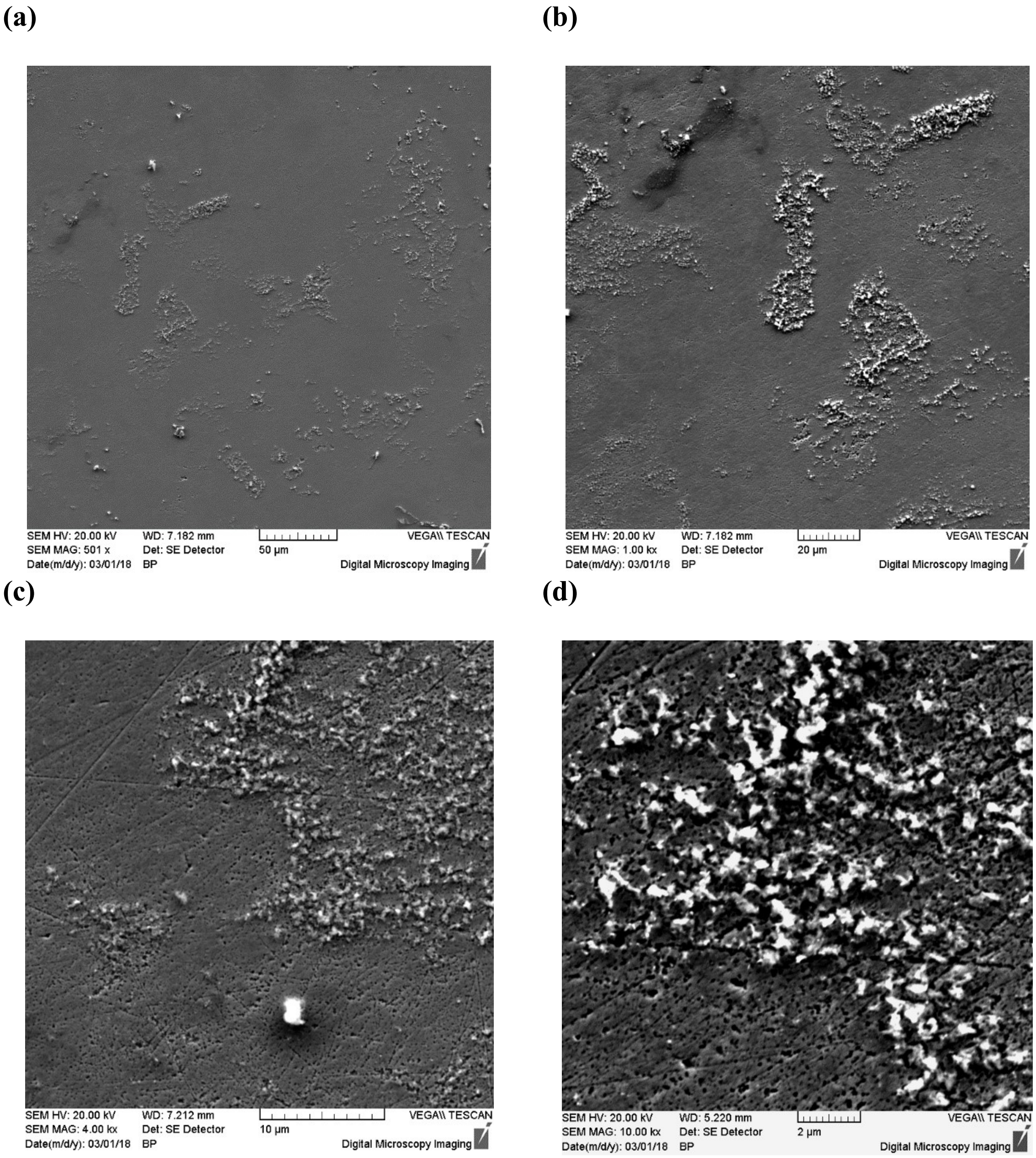

Figure 5.3**:** SEM images presenting surface morphology of deposit on the platinum working electrode. CA performed for 2 hours at -2.0V at 80 C. Magnification **(a)** 500x **(b)** 1,000x **(c)** 4,000x **(d)** 10,000x.

Two films are deposited on the surface of the platinum electrode, as shown in Figures 5.3a-c. Both films cover the entire electrode surface, however the darker film underneath and is only shown in small regions. Examining Figure 5.3d the dark film can be seen on and around the sides of the scratches located on the electrode. This indicates that the dark film is actually is a film not the base metal of the electrode. Gaseous product formation during the reduction of lanthanum is shown by tiny pits everywhere on the film. This gaseous product could be the electrogeneration of hydrogen gas from moisture adsorbed into ionic liquid from the open atmosphere, ethanol leftover from solvation step reducing to methane, or the reduction of BMIM cation to carbene. The white residue present particularly on the platinum electrode is ionic liquid that did not come off after the methanol rinse.

SEM characterization was performed on the glassy carbon at room temperature similarly to the platinum electrode. The glassy carbon working electrode was cleaned in two successive methanol baths for at least five minutes each. SEM micrographs of the electrode surface after two control experiments and ionic liquid cleaning procedure are presented below in Figures 7.4a-b.

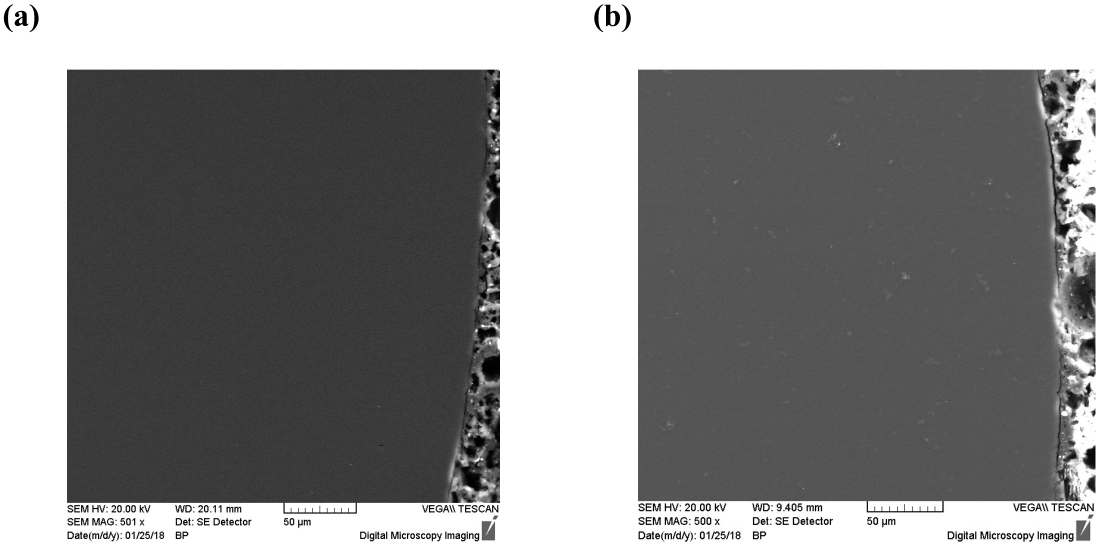

Figure 5.4: SEM images captured of electrode surface after control test **(a)** CA -3.0 for 10sec in EMIM-DCA **(b)** Electrode placed in EMIM-DCA-LaCl$_3$ for 10 min.

First experiment was a run on pure EMIM-DCA at -3.0V for deposition time (Figure 5.4a). Notice that there was no film formation indicating that the film deposited was not EMIM cation or an organic compound from the ionic liquid. For the second control experiment, the electrode placed in EMIM-DCA-LaCl$_3$ for 10 min without any electrochemistry performed (Figure 5.4b).This also does not show a film, which indicates that there must be a diving force for film formation and that our cleaning method works to remove excess ionic liquid.

Figure 5.5a-b below present electron micrographs of the glassy carbon electrode after CA performed in EMIM-DCA with $LaCl_3$. This electrode was polarized for 20 sec at -3.5 V. The electron micrograph of the film deposited on the glassy carbon electrode does not provide total coverage at this potential do to gaseous product formation during the deposition process.

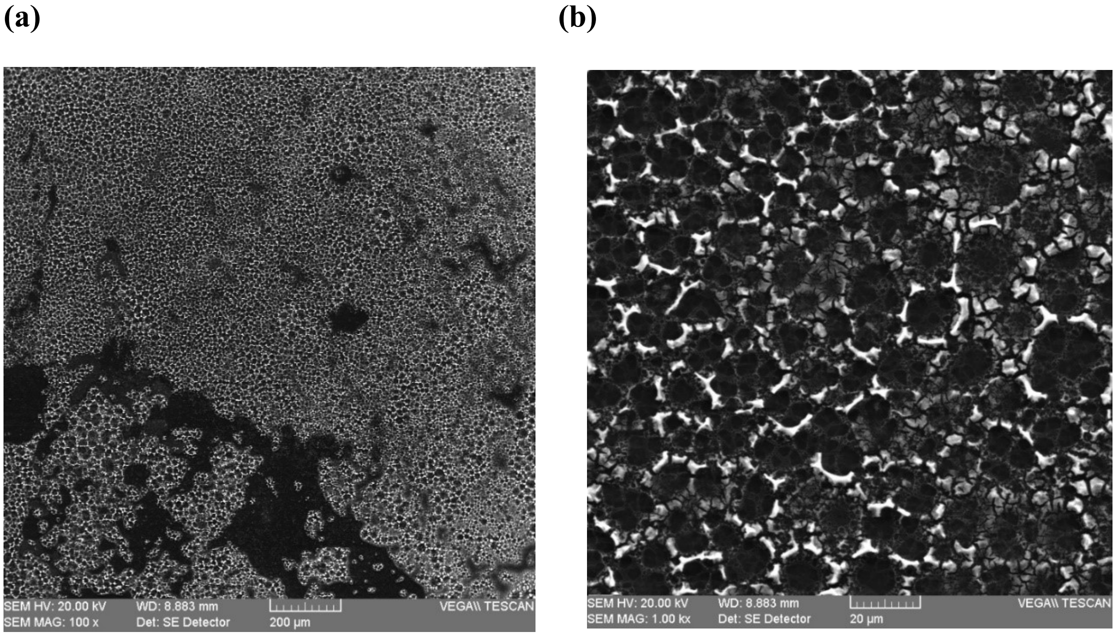

Figure 5.5**:** SEM images presenting surface morphology of deposit on the glassy carbon working electrode. CA performed for 20 sec at -3.5V at room temperature. Magnification **(a)** 100x **(b)** 1,000x**.**

Similar to the high temperature experiments performed on platinum, SEM characterization at high temperatures was performed on the glassy carbon. Figure 5.6a-c below present electron micrographs of the glassy carbon working electrode after CA performed in BMIM-DCA with $LaCl_3$. This electrode was polarized at -2.0 V for 1 hour with the temperature increased to 80° C.

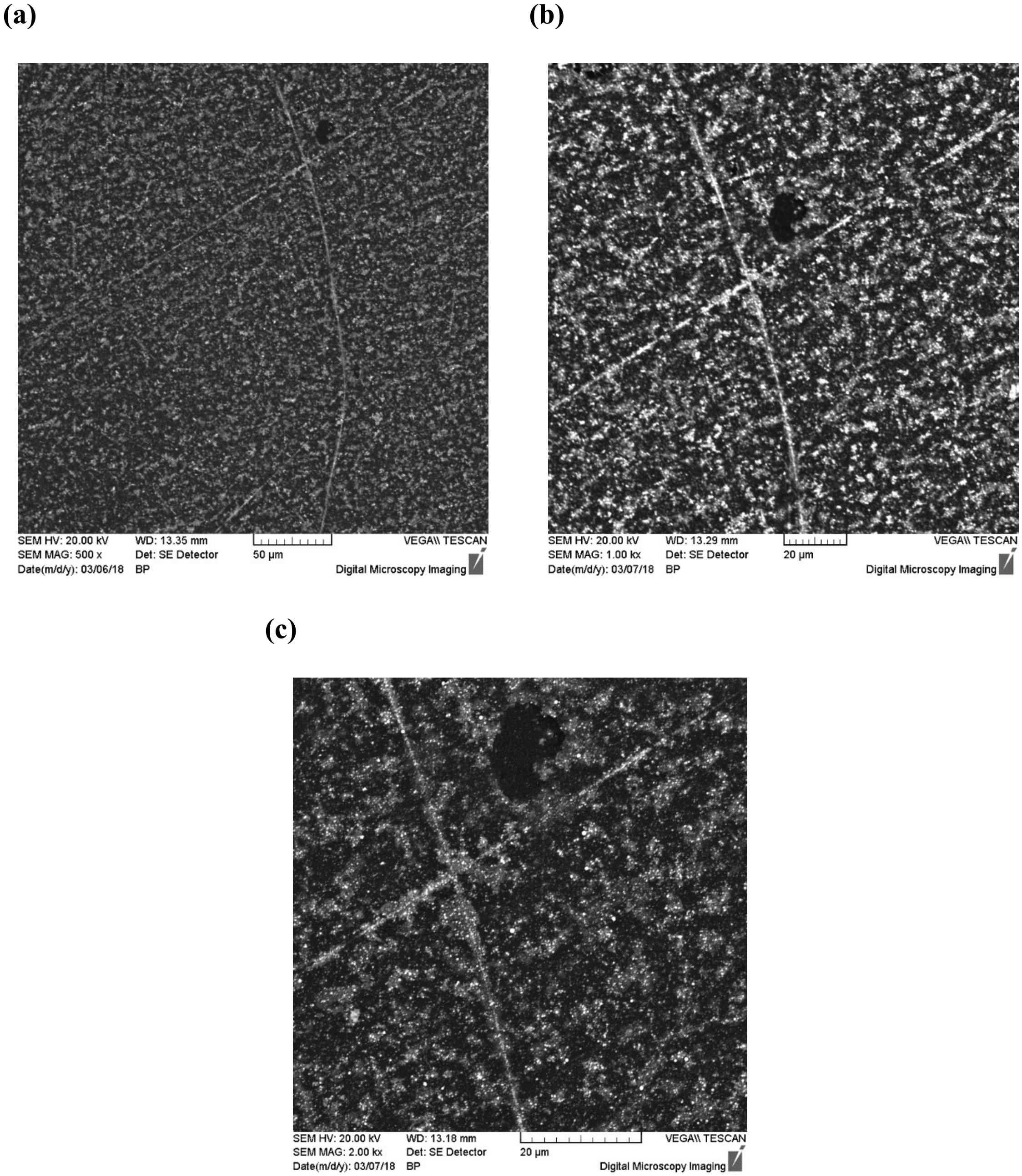

Figure 5.6**:** SEM images presenting surface morphology of deposit on the glassy carbon working electrode. CA performed for 1 hours at -2.0V at 80 C. Magnification **(a)** 500x **(b)** 1,000x **(c)** 2,000x.

In Figures 5.6a-c, notice the many tightly clustered spheres especially those that line the scratch. These spheres are consistent with metallic nucleation which is drawn to scratches on the electrode surface. Scratches on an electrode surface provide the highest energy density, thus nucleation starts and occurs more often along the scratches.

The electron micrographs of the film deposited on the brass electrode are shown in (Figure 5.7). Evidence of cracks was noted on the film of the brass electrode. We propose that these cracks arise from the generation of bubbles (hydrogen gas) at the electrodes grain boundaries (enrich Cu zones). These bubbles eventually pit and crack the film as they escape. The initial cracks lead to high energy density regions causing the creaks to widen as more bubbles are generated.

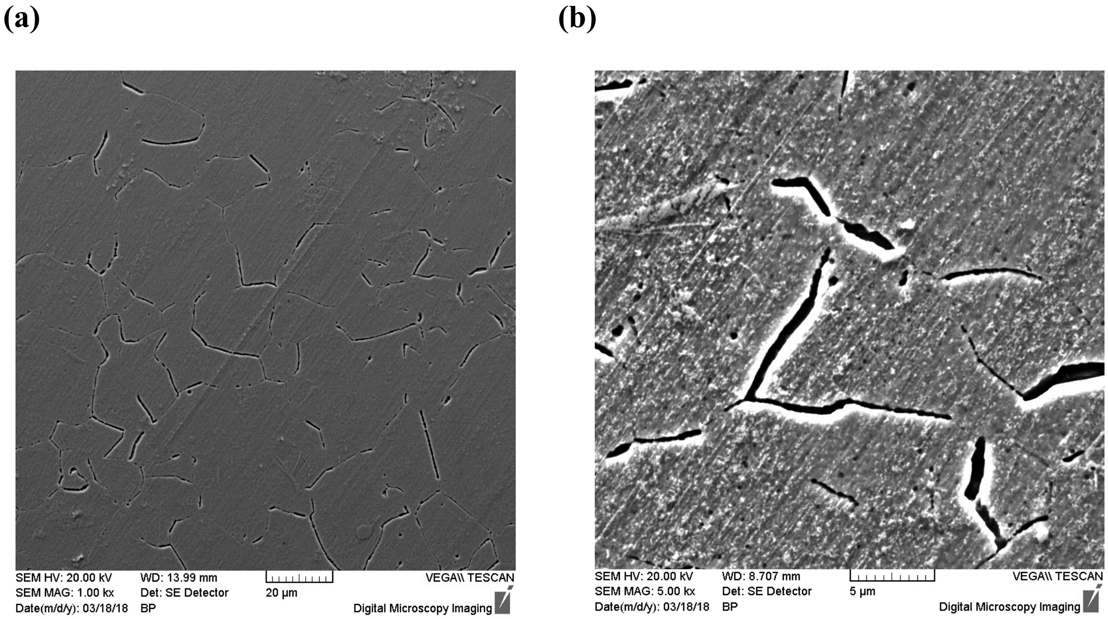

Figure 5.7**:** SEM images presenting surface morphology of deposit on the brass working electrode. CV performed 0V to -2V at 80C. Magnification **(a)** 100x **(b)** 1,000x**.**

5.3 XRD Characterization

The propose of Figure 5.8 was to show that we attempted x-ray diffraction to characterize the film. The XRD (Seimens 5000) used was effective enough to confirm that the film is lanthanum not an organic compound. Table 5.1 shows the two theta for HCP lanthanum from Spedding et al,. [40] note that the peaks' 2 thetas in the Figure 5.8 are very close to the values demonstrated by the red lines.

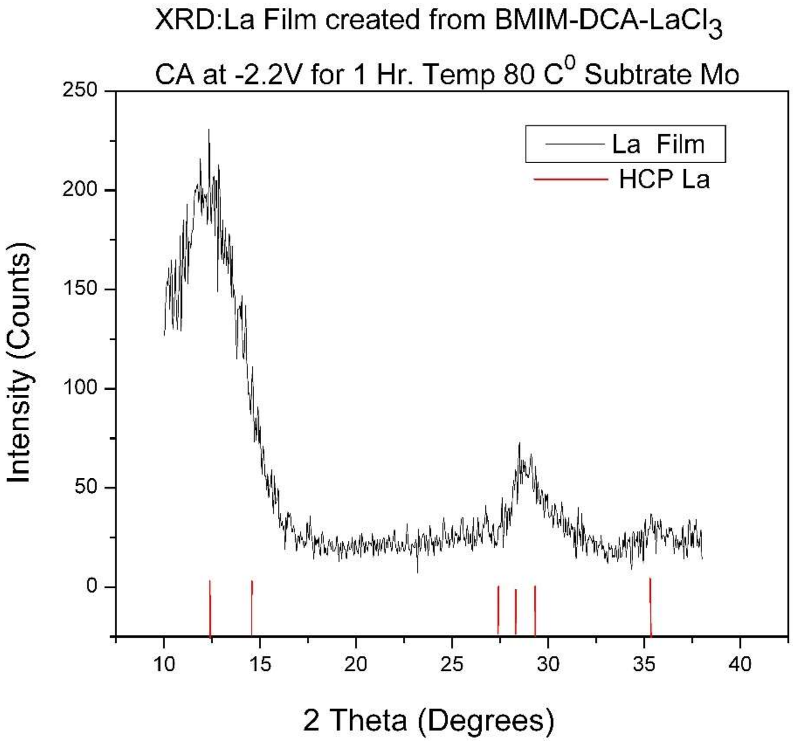

Figure 5.8**:** XRD characterizing the surface morphology of deposit as La on the Mo working electrode. CA performed for 1 hour at -2.2V at 80 C.

Table 5.1 Two Theta Values for HCP Lanthanum [40].

Lanthanum 2θ
14.57
27.32
28.3
29.38
31.09
35.3

CHAPTER 6 FUTURE WORK

To continue this research, I would recommend performing cyclic voltammetry on various electrode surfaces to analyze the influence of electrode surface on the deposition mechanism, film morphology, and electrochemical reactions. It would also be beneficial to perform RDE studies at different temperatures and La concentration on film deposition from DCA based ionic liquids. RDE experiments at different temperature, will allow one to determine the activation energy of the reaction. Performing RDE studies on EMIM-DCA with different initial concentrations of lanthanum would provide the information reaction order with respect to lanthanum.

More careful XRD characterization should also be done on the films deposited after both potentiodynamic and potentiostatic experiments. Because films deposited on the electrodes are very thin, a specialized type XRD, glazing XRD would be required for characterization such as glancing angle XRD. The chemical composition of the lanthanum films should also be analyzed by EDX spectroscopy.

CHAPTER 7 CONCLUSIONS

The primary objective of the research was to study the electrochemistry of lanthanum in ionic liquids. Lanthanum deposited from EMIM-DCA, was proven to be stable with moisture and ethanol. Background electrochemistry was performed on EMIM-DCA with and without $LaCl_3$ by cyclic voltammetry. $LaCl_3$ precipitates were formed when water was added to EMIM-DCA-$LaCl_3$ but when ethanol was added no reactions occurred. Morphology of film was examined with optical microscopy which showed that the cathodic limit of EMIM-DCA-$LaCl_3$ was about -1.8V vs Ag/AgCl. Rotating disk studies showed that both water and lanthanum reactions in EMIM-DCA had mixed kinetics.

- Cyclic voltammetry demonstrated the electrochemical stability of DCA ILs in open atmosphere.
- Ethanol was demonstrated to be an effective solvent for $LaCl_3$ and created no adverse electrochemical effects when added to DCA ionic liquids.

- EMIM and BMIM electrochemically reduced to form carbene.
- The addition of water to EMIM-DCA-$LaCl_3$ showed an irreversible reaction between water and lanthanum.
- The rotating disk studies revealed that the reduction of La in DCA ILs was not controlled purely by mass transfer.

- SEM and Optical analysis showed film formation only with the presence of lanthanum.
- XRD was conclusive that the film contains metallic lanthanum

REFERENCES

[1] Walden, P. (1914). Molecular weights and electrical conductivity of several fused salts. Bull. Acad. Imper. Sci.(St. Petersburg), 1800

[2] Hurley, F. H., & WIer, T. P. (1951). The electrodeposition of aluminum from nonaqueous solutions at room temperature. Journal of the Electrochemical Society, 98(5), 207-212.

[3] Robinson, J., & Osteryoung, R. A. (1979). An electrochemical and spectroscopic study of some aromatic hydrocarbons in the room temperature molten salt system aluminum chloride-n-butylpyridinium chloride. Journal of the American Chemical Society, 101(2), 323-327.

[4] Wilkes, J. S., Levisky, J. A., Wilson, R. A., & Hussey, C. L. (1982). Dialkylimidazolium chloroaluminate melts: a new class of room-temperature ionic liquids for electrochemistry, spectroscopy and synthesis. *Inorganic Chemistry*, *21*(3), 1263-1264

[5] Ohno, H. (Ed.). (2005). Electrochemical aspects of ionic liquids. John Wiley & Sons., 1-21, 111-116, 124-125

[6] Endres, F., Abbot, A., & MacFarlane, D. (2008). Electrodeposition from Ionic Liquids, Wiley-VCH. Electrodeposition from Ionic Liquids, Wiley-VCH.

[7] Johnson, K. E. (2007). What's an ionic liquid?. Interface-Electrochemical Society, 16(1), 38-41.

[8] Messadi, A., Mohamadou, A., Boudesocque, S., Dupont, L., Fricoteaux, P., Nguyen-Van-Nhien, A., & Courty, M. (2013). Syntheses and characterisation of hydrophobic ionic liquids containing trialkyl (2-ethoxy-2-oxoethyl) ammonium or N-(1-methylpyrrolidyl-2-ethoxy-2-oxoethyl) ammonium cations. *Journal of Molecular Liquids*, *184*, 68-72.

[9] Wankowski, J. L. (2017). Fundamental Studies of Metal Ion Extraction into Ionic Liquids By Macrocyclic Polyethers(Doctoral dissertation, The University of Wisconsin-Milwaukee).

[10] Díaz-Delgado, R., & Doherty, A. P. (2016). Carbons, ionic liquids, and quinones for electrochemical capacitors. *Frontiers in Materials*, *3*, 18.

[11] de María, P. D., & Maugeri, Z. (2011). Ionic liquids in biotransformations: from proof-of-concept to emerging deep-eutectic-solvents. *Current opinion in chemical biology*, *15*(2), 220-225.

[12] Endres, F. (2002). Ionic liquids: solvents for the electrodeposition of metals and semiconductors. ChemPhysChem, 3(2), 144-154.

[13] Abbott, A. P., Ryder, K. S., & König, U. (2008). Electrofinishing of metals using eutectic based ionic liquids. Transactions of the IMF, 86(4), 196-204.

[14] Gorke, J., Srienc, F., & Kazlauskas, R. (2010). Toward advanced ionic liquids. Polar, enzyme-friendly solvents for biocatalysis. Biotechnology and Bioprocess Engineering, 15(1), 40-53.

[15] Hajipour, A. R., & Rafiee, F. (2009). Basic ionic liquids. A short review. Journal of the Iranian Chemical Society, 6(4), 647-678.

[16] Anastas, P. T., & Kirchhoff, M. M. (2002). Origins, current status, and future challenges of green chemistry. Accounts of chemical research, 35(9), 686-694

[17] Mantz,RA. and Trulove PC., (2008) Viscosity and density of ionic liquids, in Ionic Liquids in Synthesis, e Wasserscheid ,P; Welton, T. Wiley-VCH, Weinheim, , 72–88

[18] Asenbauer, J., Hassen, N. B., McCloskey, B. D., & Prausnitz, J. M. (2017). Solubilities and ionic conductivities of ionic liquids containing lithium salts. *Electrochimica Acta*, *247*, 1038-1043.

[19] Deng, M. J., Sun, I. W., Chen, P. Y., Chang, J. K., & Tsai, W. T. (2008). Electrodeposition behavior of nickel in the water-and air-stable 1-ethyl-3-methylimidazolium-dicyanamide room-temperature ionic liquid. Electrochimica Acta, 53(19), 5812-5818.

[20] Simons, T. J., Howlett, P. C., Torriero, A. A. J., MacFarlane, D. R., & Forsyth, M. (2013). Electrochemical, transport, and spectroscopic properties of 1-ethyl-3-methylimidazolium ionic liquid electrolytes containing zinc dicyanamide. *The Journal of Physical Chemistry C*, *117*(6), 2662-2669

[21] Vanderaspoilden, S., Christophe, J., Doneux, T., & Buess-Herman, C. (2015). Contrasted electrochemical behaviour of Cu (I) and Cu (II) ions in 1-butyl-3-methylimidazolium dicyanamide. Electrochimica acta, 162, 156-162.

[22] Simons, T. J., Howlett, P. C., Torriero, A. A. J., MacFarlane, D. R., & Forsyth, M. (2013). Electrochemical, transport, and spectroscopic properties of 1-ethyl-3-methylimidazolium ionic liquid electrolytes containing zinc dicyanamide. *The Journal of Physical Chemistry C*, *117*(6), 2662-2669.

[23] Begg, C. G., Grimmett, M. R., & Yu-Man, L. (1973). The synthesis of 2-alkyl-and 2-acyl-imidazoles by substitution methods. Australian Journal of Chemistry, 26(2), 415-420.

[24] Lane, G. H. (2012). Electrochemical reduction mechanisms and stabilities of some cation types used in ionic liquids and other organic salts. *Electrochimica Acta*, *83*, 513-528.

[25] Bard, A. J., Faulkner, L. R., Leddy, J., & Zoski, C. G. (1980). Electrochemical methods: fundamentals and applications (Vol. 2). New York: wiley

[26] Matsumiya,M.,Kikuchi,Y.,Yamada,T.,Kawakami,S., (2014) Extraction of rare earth ion by tri-n-butylphosphate/phoshonium ionic liquids and the feasibility of recovery by direct electrodeposition, sepration and Purification Technology 130, 91-101

[27] Sengupta, A., Murali, M. S., & Mohapatra, P. K. (2014). Electrochemical behavior of cerium (IV) in a RTIL and its mixture with ethanol. *Journal of Rare Earths*, *32*(7), 641-647

[28] Pan, Y., & Hussey, C. L. (2013). Electrochemical and Spectroscopic Investigation of Ln3+ (Ln= Sm, Eu, and Yb) Solvation in Bis (trifluoromethylsulfonyl) imide-Based Ionic Liquids and Coordination by N, N, N′, N′-Tetraoctyl-3-oxa-pentane Diamide (TODGA) and Chloride. Inorganic chemistry, 52(6), 3241-3252.

[29] Chou, L. H., & Hussey, C. L. (2014). An electrochemical and spectroscopic study of Nd (III) and Pr (III) coordination in the 1-butyl-1-methylpyrrolidinium bis (trifluoromethylsulfonyl) imide ionic liquid containing chloride ion. Inorganic chemistry, 53(11), 5750-5758

[30] Legeai, S., Diliberto, S., Stein, N., Boulanger, C., Estager, J., Papaiconomou, N., & Draye, M. (2008). Room-temperature ionic liquid for lanthanum electrodeposition. *Electrochemistry Communications*, *10*(11), 1661-1664.

[31] Bourbos, E., Giannopoulou, I., Karantonis, A., Paspaliaris, I., & Panias, D. (2015). Electrodeposition of Rare Earth Metals from Ionic Liquids. In Rare Earths Industry ,199-207.

[32] Zhang, Q. B., Yang, C., Hua, Y. X., Li, Y., & Dong, P. (2015). Electrochemical preparation of nanostructured lanthanum using lanthanum chloride as a precursor in 1-butyl-3-methylimidazolium dicyanamide ionic liquid. Physical Chemistry Chemical Physics, 17(6), 4701-4707.

[33] Fisher., Linear Sweep and Cyclic Voltammetry: The Principles." Department of Chemical Engineering and Biotechnology, 16 Dec. 2013

[34] V. G. Levich, (1962) Physicochemical Hydrodynamics, 2nd. Ed., Prentice-Hall, Englewood Cliffs, N. J., 60 -72.

[35] Bockris, J. M., Drazic, D., & Despic, A. R. (1961). The electrode kinetics of the deposition and dissolution of iron. Electrochimica Acta, 4(2-4), 325-361

[36] B. Pesic, (2016) Advanced Electrochemical Separations of Actinide/Fission Products via the Control of Nucleation and Growth of Electrodeposits, US Department of Energy, DOE-NEUP Award Number DE-NE00008556

[37] Bhatt, A. I., & Snook, G. A. (2013). Reference electrodes for ionic liquids and molten salts. In Handbook of reference electrodes (pp. 189-227). Springer Berlin Heidelberg.

[38] Giaccherini, A., & Lavacchi, A. Modelling of the rotating disk electrode in Ionic liquids: difference between water based and ionic liquids electrolytes.

[39] Schmidt, V.M., Ianniello, R., Pastor, E., Gonzalez, S., (1996) Electrochemical reactivity of ethanol on porous Pt and PtRu; Oxidation/Reduction reaction in 1 M $HClO_4$, Journal of Physical Chemistry 100 17901-17908.

[40] Lanthanum: Spedding F H, Daane A H, Herrmann K W Acta Crystallographica 9 (1956) 559-563, The crystal structures and lattice parameters of high-purity scandium,yttrium and the rare earth metals